



Observation of a narrow pentaquark state, $P_c(4312)^+$, and of two-peak structure of the $P_c(4450)^+$

LHCb collaboration[†]

Abstract

A narrow pentaquark state, $P_c(4312)^+$, decaying to $J/\psi p$ is discovered with a statistical significance of 7.3σ in a data sample of $\Lambda_b^0 \rightarrow J/\psi p K^-$ decays which is an order of magnitude larger than that previously analyzed by the LHCb collaboration. The $P_c(4450)^+$ pentaquark structure formerly reported by LHCb is confirmed and observed to consist of two narrow overlapping peaks, $P_c(4440)^+$ and $P_c(4457)^+$, where the statistical significance of this two-peak interpretation is 5.4σ . Proximity of the $\Sigma_c^+ \bar{D}^0$ and $\Sigma_c^+ \bar{D}^{*0}$ thresholds to the observed narrow peaks suggests that they play an important role in the dynamics of these states.

Accepted by Phys. Rev. Lett.

© 2019 CERN for the benefit of the LHCb collaboration. CC-BY-4.0 licence.

[†]Authors are listed at the end of this paper.

A major turning point in exotic baryon spectroscopy was achieved at the Large Hadron Collider when, from an analysis of Run 1 data, the LHCb collaboration reported the observation of significant $J/\psi p$ pentaquark structures in $\Lambda_b^0 \rightarrow J/\psi p K^-$ decays (inclusion of charge-conjugate processes is implied throughout). A model-dependent six-dimensional amplitude analysis of invariant masses and decay angles describing the Λ_b^0 decay revealed a $P_c(4450)^+$ structure peaking at $4449.8 \pm 1.7 \pm 2.5$ MeV with a width of $39 \pm 5 \pm 19$ MeV and a fit fraction of $(4.1 \pm 0.5 \pm 1.1)\%$ [1]. Even though not apparent from the $m_{J/\psi p}$ distribution alone, the amplitude analysis also required a second broad $J/\psi p$ state to obtain a good description of the data, which peaks at $4380 \pm 8 \pm 29$ MeV with a width of $205 \pm 18 \pm 86$ MeV and a fit fraction of $(8.4 \pm 0.7 \pm 4.2)\%$. Furthermore, the exotic hadron character of the $J/\psi p$ structure near 4450 MeV was demonstrated in a model-independent way in Ref. [2], where it was shown to be too narrow to be accounted for by $\Lambda^* \rightarrow p K^-$ reflections (Λ^* denotes Λ excitations). Various interpretations of these structures have been proposed, including tightly bound $duuc\bar{c}$ pentaquark states [3–9], loosely bound molecular baryon-meson pentaquark states [10–15], or peaks due to triangle-diagram processes [16–19].

In this Letter, an analysis is presented of $\Lambda_b^0 \rightarrow J/\psi p K^-$ decays based on the combined data set collected by the LHCb collaboration in Run 1, with pp collision energies of 7 and 8 TeV corresponding to a total integrated luminosity of 3 fb^{-1} , and in Run 2 at 13 TeV corresponding to 6 fb^{-1} . The LHCb detector is a single-arm forward spectrometer covering the pseudorapidity range $2 < \eta < 5$, described in detail in Refs. [20, 21]. The data selection is similar to that used in Ref. [1]. However, in this updated analysis, the hadron-identification information is included in the Boosted Decision Tree (BDT) discriminant, which increases the Λ_b^0 signal efficiency by almost a factor of two while leaving the background level almost unchanged. The resulting sample contains 246k $\Lambda_b^0 \rightarrow J/\psi p K^-$ decays (see the Supplemental Material to this Letter), which is nine times more than used in the Run 1 analyses [1, 2].

When this combined data set is fit with the same amplitude model used in Ref. [1], the $P_c(4450)^+$ and $P_c(4380)^+$ parameters are found to be consistent with the previous results. However, this should be considered only as a cross check, since analysis of this much larger data sample reveals additional peaking structures in the $J/\psi p$ mass spectrum, which are too small to have been significant before (see Fig. 1 left). A narrow peak is observed near 4312 MeV with a width comparable to the mass resolution. The structure at 4450 MeV is now resolved into two narrow peaks at 4440 and 4457 MeV, which are more visible when the dominant $\Lambda^* \rightarrow p K^-$ contributions, which peak at low $p K^-$ masses (m_{Kp}) as shown in Fig. 1 right and Fig. 2, are suppressed by requiring $m_{Kp} > 1.9$ GeV (see Fig. 3). This m_{Kp} requirement maximizes the expected signal significance for P_c^+ states that decay isotropically.

Performing a rigorous amplitude analysis of this new data sample is computationally challenging. The $m_{J/\psi p}$ mass resolution must be taken into account, and the size of the data sample to fit has greatly increased. Formulating an amplitude model whose systematic uncertainties are comparable to the statistical precision provided by this larger data sample is difficult given the large number of Λ^* excitations [22, 23], coupled-channel effects [24], and the possible presence of one or more wide P_c^+ contributions, like the previously reported $P_c(4380)^+$ state. Fortunately, the newly observed peaks are so narrow that it is not necessary to construct an amplitude model to prove that these states are not artifacts of interfering Λ^* resonances [2].

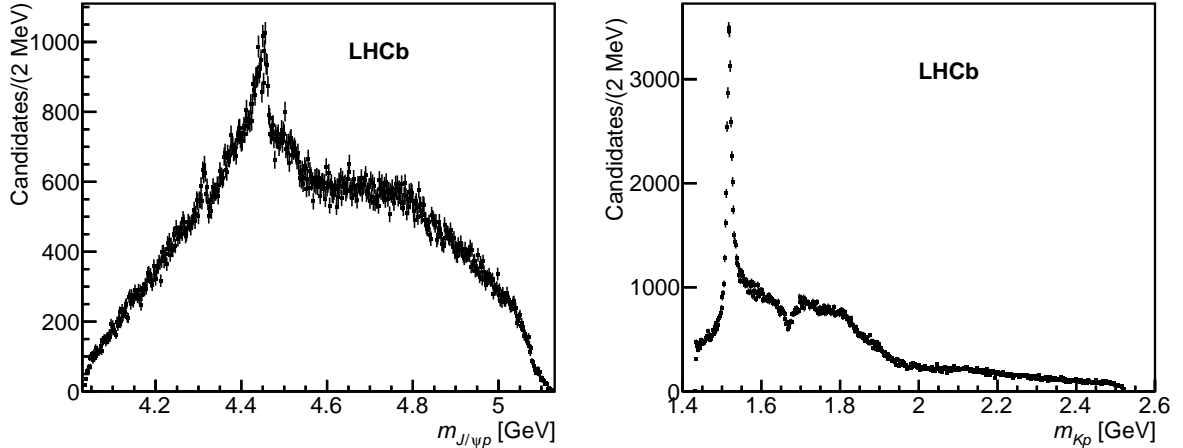


Figure 1: Distribution of (left) $m_{J/\psi p}$ and (right) m_{Kp} for $\Lambda_b^0 \rightarrow J/\psi p K^-$ candidates. The prominent peak in m_{Kp} is due to the $\Lambda(1520)$ resonance.

Binned χ^2 fits are performed to the one-dimensional $m_{J/\psi p}$ distribution in the range $4.22 < m_{J/\psi p} < 4.57$ GeV to determine the masses (M), widths (Γ), and relative production rates (\mathcal{R}) of the narrow P_c^+ states under the assumption that they can be described by relativistic Breit–Wigner (BW) amplitudes. These $m_{J/\psi p}$ fits alone cannot distinguish broad P_c^+ states from other contributions that vary slowly with $m_{J/\psi p}$. Therefore, a verification of the $P_c(4380)^+$ state observed in Ref. [1] awaits completion of an amplitude analysis of this new larger data set.

Many variations of the $m_{J/\psi p}$ fits are performed to study the robustness of the measured P_c^+ properties. The $m_{J/\psi p}$ distribution is fit both with and without requiring $m_{Kp} > 1.9$ GeV, which removes over 80% of the Λ^* contributions. In addition, fits are performed on the $m_{J/\psi p}$ distribution obtained by applying $\cos\theta_{P_c}$ -dependent weights to each candidate to enhance the P_c^+ signal, where θ_{P_c} is the angle between the K^- and J/ψ in the P_c^+ rest frame (the P_c^+ helicity angle [1]). The Λ^* contributions mostly populate the $\cos\theta_{P_c} > 0$ region. The weights are taken to be the inverse of the expected background at each $\cos\theta_{P_c}$, which is approximately given by the density of candidates observed in data since the signal contributions are small. The weight function is shown in Fig. 4. The best sensitivity to P_c^+ contributions is obtained from the $\cos\theta_{P_c}$ -weighted $m_{J/\psi p}$ distribution, followed by the sample with the $m_{Kp} > 1.9$ GeV requirement. However, since the background composition and shape are different in the three samples, the results from all three fits are used when assessing the systematic uncertainties.

The one-dimensional fit strategy is validated on ensembles of large simulated data sets sampled from several six-dimensional amplitude models, similar to those of Ref. [1], with or without a broad P_c^+ state and considering various P_c^+ quantum-number assignments. The main conclusion from these studies is that the dominant systematic uncertainty is due to possible interference between various P_c^+ states. Such interference effects cannot be unambiguously disentangled using the $m_{J/\psi p}$ distribution alone. Therefore, fits are performed considering many possible interference configurations, with the observed variations in the P_c^+ properties assigned as systematic uncertainties.

In all fits, the $m_{J/\psi p}$ distribution is modeled by three narrow BW P_c^+ terms and a

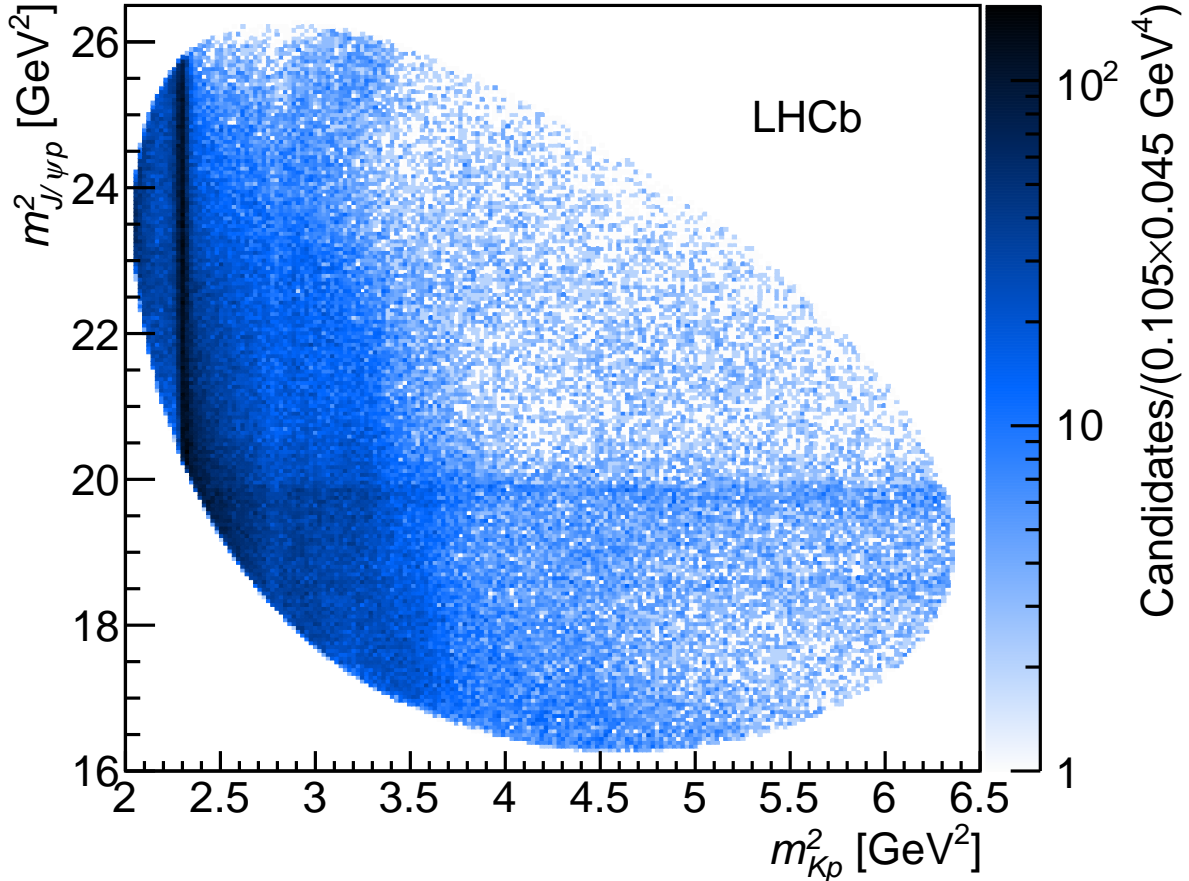


Figure 2: Dalitz plot of $\Lambda_b^0 \rightarrow J/\psi p K^-$ candidates. The data contain 6.4% of non- Λ_b^0 backgrounds, which are distributed smoothly over the phase-space. The vertical bands correspond to the Λ^* resonances. The horizontal bands correspond to the $P_c(4312)^+$, $P_c(4440)^+$, and $P_c(4457)^+$ structures at $m_{J/\psi p}^2 = 18.6, 19.7,$ and 19.9 GeV^2 , respectively.

smooth parametrization of the background. Here, background refers to Λ^* reflections, small non- Λ_b^0 contributions (which comprise 6.4% of the sample), and possibly additional broad P_c^+ structures. Many different background parametrizations are considered (discussed below), each of which is found to produce negligible bias in the P_c^+ parameters in the validation fits. Each fit component is multiplied by a phase-space factor, $p \cdot q$, where p (q) is the break-up momentum in the $\Lambda_b^0 \rightarrow P_c^+ K^-$ ($P_c^+ \rightarrow J/\psi p$) decay. Since the signal peaks are narrow, all fit components are convolved with the detector resolution, which is 2–3 MeV in the fit region (see the Supplemental Material). Finally, the detection efficiency has negligible impact on the signal $m_{J/\psi p}$ distributions, and therefore, is not considered in these fits.

In the nominal fits, the BW contributions are added incoherently. The results of these fits are displayed in Fig. 5 for two parametrizations of the background: one using a high-order polynomial; and another using a low-order polynomial, along with an additional wide P_c^+ BW term whose mass and width are free to vary in the fits. For both background parametrizations, a range of polynomial orders is considered. The lowest order used for each case is the smallest that adequately describes the data, which is found to correspond

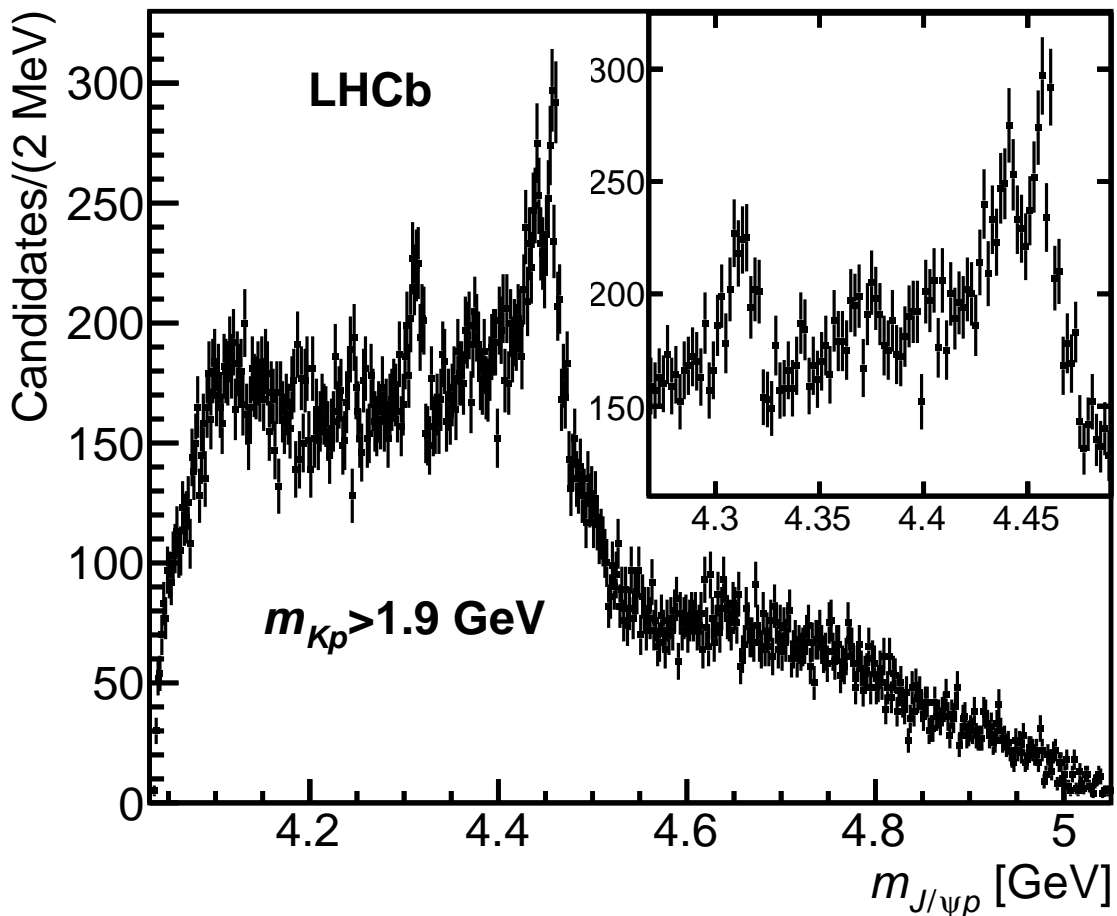


Figure 3: Distribution of $m_{J/\psi p}$ from $\Lambda_b^0 \rightarrow J/\psi p K^-$ candidates after suppression of the dominant $\Lambda^* \rightarrow p K^-$ contributions with the $m_{Kp} > 1.9$ GeV requirement. The inset shows a zoom into the region of the narrow P_c^+ peaks.

to the minimum order required to obtain unbiased P_c^+ estimators in the fit-validation studies in the absence of interference. The highest orders are chosen such that the background model is capable of describing any structures that could be produced by either non- P_c^+ or broad- P_c^+ contributions. Figure 6 shows the fit from which the central values of the P_c^+ properties are obtained, while the background-model-dependent variations observed in these properties are included in the systematic uncertainties. The fits with and without the broad P_c^+ state both describe the data well. Therefore, these fits can neither confirm nor contradict the existence of the $P_c(4380)^+$ state.

To determine the significance of the $P_c(4312)^+$ state, the change of the fit χ^2 when adding this component is used as the test statistic, where the distribution under the null hypothesis is obtained from a large ensemble of pseudoexperiments. The p -value, expressed in Gaussian standard deviations, corresponds to 7.6σ (8.5σ) for the fits to the $m_{Kp} > 1.9$ GeV ($\cos\theta_{Pc}$ -weighted) distribution, ignoring the look-elsewhere effect. To account for this effect, the $m_{J/\psi p}$ distribution in each pseudoexperiment is scanned to find the most significant narrow and isolated peak (excluding the 4450 MeV peak region). This method lowers the $P_c(4312)^+$ significance to 7.3σ (8.2σ).

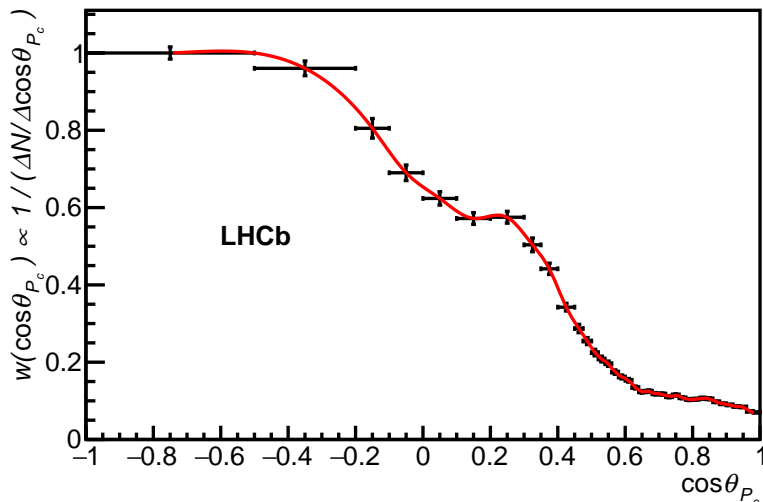


Figure 4: Weight function $w(\cos\theta_{P_c})$ applied to candidates, determined as the inverse of the density of Λ_b^0 candidates in the narrow P_c^+ peak region. The red line is a spline function used to interpolate between bin centers.

To evaluate the significance of the two-peak structure versus the one-peak interpretation of the 4450 MeV region, the null hypothesis uses just one BW to encompass both the $P_c(4440)^+$ and $P_c(4457)^+$ peaks (the fit also includes the $P_c(4312)^+$ BW), which gives $P_c(4450)^+$ mass and width values that are consistent with those obtained from the amplitude analysis of Ref. [1]. Pseudoexperiments are again used to determine the $\Delta\chi^2$ distribution under the null hypothesis. The significance of the two-peak structure is 5.4σ (6.2σ) for the $m_{Kp} > 1.9$ GeV ($\cos\theta_{P_c}$ -weighted) samples. This significance is large enough to render the single peak interpretation of the 4450 MeV region obsolete. Therefore, the results presented here for this structure supersede those previously presented in Ref. [1] (see the Supplemental Material for more detailed discussion). To investigate the systematic uncertainties on P_c^+ properties due to interference, which can only be important for P_c^+ resonances with the same spin and parity, fits to the $\cos\theta_{P_c}$ -weighted distribution are repeated using various coherent sums of two of the BW amplitudes. Each of these fits includes a phase between interfering resonances as an extra free parameter. None of the interference effects studied is found to produce a significant $\Delta\chi^2$ relative to the fits using an incoherent sum of BW amplitudes. However, substantial shifts in the P_c^+ properties are observed, and are included in the systematic uncertainties. For example, in such fit the $P_c(4312)^+$ mass increases, while its width is rather stable, leading to a large positive systematic uncertainty of 6.8 MeV on its mass.

As in Ref. [1], the Λ_b^0 candidates are kinematically constrained to the known J/ψ and Λ_b^0 masses [25], which substantially improves the $m_{J/\psi p}$ resolution and determines the absolute mass scale with an accuracy of 0.2 MeV. The mass resolution is known with a 10% relative uncertainty. Varying this within its uncertainty changes the widths of the narrow states in the nominal fit by up to 0.5 MeV, 0.2 MeV, and 0.8 MeV for the $P_c(4312)^+$, $P_c(4440)^+$, and $P_c(4457)^+$ states, respectively. The widths of all three narrow P_c^+ peaks are consistent with the mass resolution within the systematic uncertainties. Therefore, upper limits are placed on their natural widths at the 95% confidence level (CL), which account for the uncertainty on the detector resolution and in the fit model.

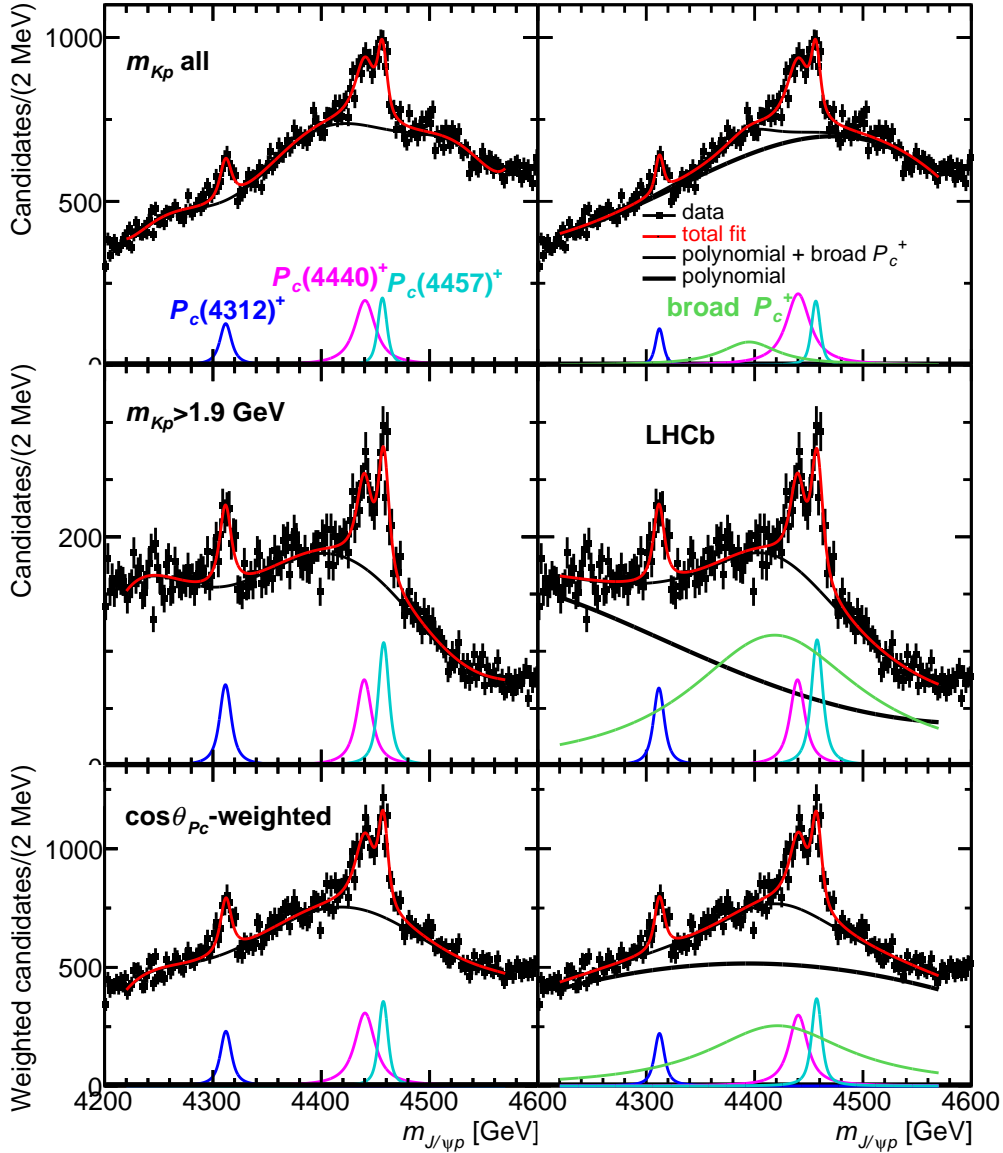


Figure 5: Fits to the $m_{J/\psi p}$ distributions of the (top row) inclusive, (middle row) $m_{Kp} > 1.9$ GeV, and (bottom row) $\cos\theta_{Pc}$ -weighted samples with three incoherently summed BW amplitudes representing the narrow P_c^+ signals on top of a (left column) high-order polynomial function or (right column) lower-order polynomial plus a broad P_c^+ state represented by a fourth BW amplitude.

A number of additional fits are performed when evaluating the systematic uncertainties. The nominal fits assume S-wave (no angular momentum) production and decay. Including P-wave factors in the BW amplitudes has negligible effect on the results. In addition to the nominal fits with three narrow peaks in the $4.22 < m_{J/\psi p} < 4.57$ GeV region, fits including only the $P_c(4312)^+$ are performed in the narrow 4.22–4.44 GeV range. Fits are also performed using a data sample selected with an alternative approach, where no BDT is used resulting in about twice as much background.

The total systematic uncertainties assigned on the mass and width of each narrow P_c^+

Table 1: Summary of P_c^+ properties. The central values are based on the fit displayed in Fig. 6.

State	M [MeV]	Γ [MeV]	(95% CL)	\mathcal{R} [%]
$P_c(4312)^+$	$4311.9 \pm 0.7^{+6.8}_{-0.6}$	$9.8 \pm 2.7^{+3.7}_{-4.5}$	(< 27)	$0.30 \pm 0.07^{+0.34}_{-0.09}$
$P_c(4440)^+$	$4440.3 \pm 1.3^{+4.1}_{-4.7}$	$20.6 \pm 4.9^{+8.7}_{-10.1}$	(< 49)	$1.11 \pm 0.33^{+0.22}_{-0.10}$
$P_c(4457)^+$	$4457.3 \pm 0.6^{+4.1}_{-1.7}$	$6.4 \pm 2.0^{+5.7}_{-1.9}$	(< 20)	$0.53 \pm 0.16^{+0.15}_{-0.13}$

state are taken to be the largest deviations observed among all fits. These include the fits to all three versions of the $m_{J/\psi p}$ distribution, each configuration of the P_c^+ interference, all variations of the background model, and each of the additional fits just described. The masses, widths, and the relative contributions (\mathcal{R} values) of the three narrow P_c^+ states, including all systematic uncertainties, are given in Table 1.

To obtain estimates of the relative contributions of the P_c^+ states, the Λ_b^0 candidates are weighted by the inverse of the reconstruction efficiency, which is parametrized in all six dimensions of the Λ_b^0 decay phase-space (Eq. (68) in the Supplemental Material to Ref. [26]). The efficiency-weighted $m_{J/\psi p}$ distribution, without the $m_{Kp} > 1.9$ GeV requirement, is fit to determine the P_c^+ contributions, which are then divided by the efficiency-corrected and background-subtracted Λ_b^0 yields. This method makes the results independent of the unknown quantum numbers and helicity structure of the P_c^+ production and decay. Unfortunately, this approach also suffers from large Λ^* backgrounds and from sizable fluctuations in the low-efficiency regions. In these fits, the P_c^+ terms are added incoherently, absorbing any interference effects, which can be large (see, *e.g.*, Fig. S2 in the Supplemental Material), into the BW amplitudes. Therefore, the $\mathcal{R} \equiv \mathcal{B}(\Lambda_b^0 \rightarrow P_c^+ K^-) \mathcal{B}(P_c^+ \rightarrow J/\psi p) / \mathcal{B}(\Lambda_b^0 \rightarrow J/\psi p K^-)$ values reported for each P_c^+ state differ from the fit fractions typically reported in amplitude analyses, since \mathcal{R} includes both the BW amplitude squared and all of its interference terms. Similar fit variations are considered here as above, *e.g.*, different background models and selection criteria are all evaluated. The resulting systematic uncertainties on \mathcal{R} are large, as shown in Table 1.

The narrow widths of the P_c^+ peaks make a compelling case for the bound-state character of the observed states. However, it has been pointed out by many authors [16–19] that peaking structures in this $J/\psi p$ mass range can also be generated by triangle diagrams. The $P_c(4312)^+$ and $P_c(4440)^+$ peaks are unlikely to arise from triangle diagrams, due to a lack of any appropriate hadron-rescattering thresholds as discussed in more detail in the Supplemental Material. The $P_c(4457)^+$ peaks at the $\Lambda_c^+(2595)\bar{D}^0$ threshold ($J^P = 1/2^+$ in S-wave) [18], and the $D_{s1}(2860)^-$ meson is a suitable candidate to be exchanged in the corresponding triangle diagram. However, this triangle-diagram term does not describe the data nearly as well as the BW does (Fig. S5 in the Supplemental Material [27]). This possibility deserves more scrutiny within the amplitude-analysis approach.

Narrow P_c^+ states could arise by binding a narrow baryon with a narrow meson, where the separation of c and \bar{c} into distinct confinement volumes provides a natural suppression mechanism for the P_c^+ widths. The only narrow baryon-meson combinations with mass thresholds in the appropriate mass range are $p\chi_{cJ}$, $\Lambda_c^+ \bar{D}^{(*)0}$, and $\Sigma_c \bar{D}^{(*)}$ (both $\Sigma_c^+ \bar{D}^{(*)0}$ and $\Sigma_c^{++} \bar{D}^{(*)-}$ are possible, the threshold for the latter is about 5 MeV higher than the former). There is no known S-wave binding mechanism for $p\chi_{cJ}$ combinations [28] and $\Lambda_c^+ \bar{D}^{(*)0}$ interactions are expected to be repulsive, leaving only the $\Sigma_c \bar{D}^{(*)}$ pairs expected

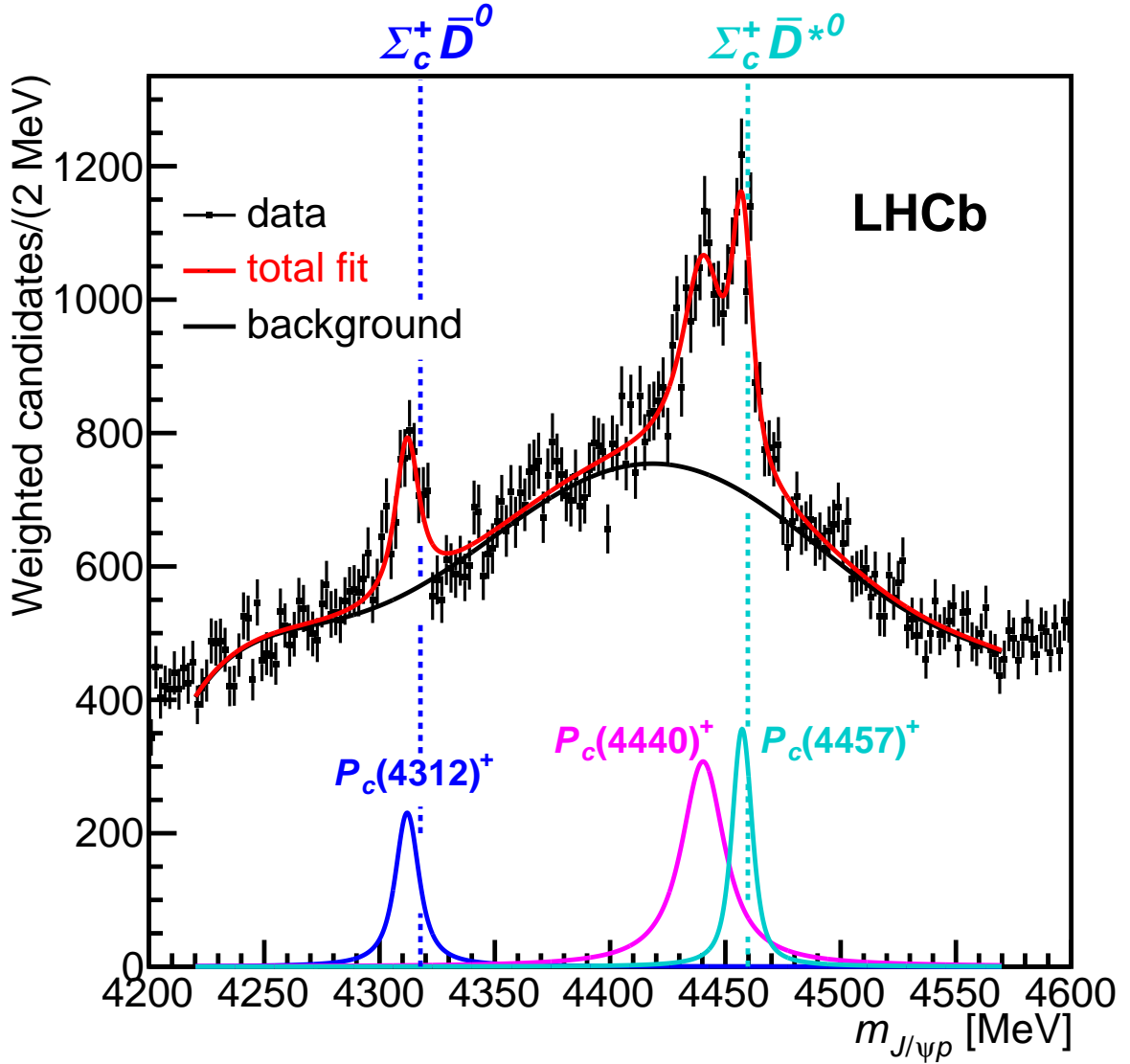


Figure 6: Fit to the $\cos\theta_{P_c}$ -weighted $m_{J/\psi p}$ distribution with three BW amplitudes and a sixth-order polynomial background. This fit is used to determine the central values of the masses and widths of the P_c^+ states. The mass thresholds for the $\Sigma_c^+ \bar{D}^0$ and $\Sigma_c^+ \bar{D}^{*0}$ final states are superimposed.

to form bound states [29–31]. The masses of the $P_c(4312)^+$ and $P_c(4457)^+$ states are approximately 5 MeV and 2 MeV below the $\Sigma_c^+ \bar{D}^0$ and $\Sigma_c^+ \bar{D}^{*0}$ thresholds, respectively, as illustrated in Fig. 6, making them excellent candidates for bound states of these systems. The $P_c(4440)^+$ could be the second $\Sigma_c \bar{D}^*$ state, with about 20 MeV of binding energy, since two states with $J^P = 1/2^-$ and $3/2^-$ are possible. In fact, several papers on hidden-charm states created dynamically by charmed meson-baryon interactions [32–34] were published well before the first observation of the P_c^+ structures [1] and some of these predictions for $\Sigma_c^+ \bar{D}^0$ and $\Sigma_c^+ \bar{D}^{*0}$ states [29–31] are consistent with the observed narrow P_c^+ states. Such an interpretation of the $P_c(4312)^+$ state (implies $J^P = 1/2^-$) would point to the importance of ρ -meson exchange, since a pion cannot be exchanged in this system [10].

In summary, the nine-fold increase in the number of $\Lambda_b^0 \rightarrow J/\psi p K^-$ decays reconstructed with the LHCb detector sheds more light onto the $J/\psi p$ structures found in this final state. The previously reported $P_c(4450)^+$ peak [1] is confirmed and resolved at 5.4σ significance into two narrow states: the $P_c(4440)^+$ and $P_c(4457)^+$ exotic baryons. A narrow companion state, $P_c(4312)^+$, is discovered with 7.3σ significance.

The minimal quark content of these states is $duuc\bar{c}$. Since all three states are narrow and below the $\Sigma_c^+ \bar{D}^0$ and $\Sigma_c^+ \bar{D}^{*0}$ ($[duc][u\bar{c}]$) thresholds within plausible hadron-hadron binding energies, they provide the strongest experimental evidence to date for the existence of bound states of a baryon and a meson. The $\Sigma_c^+ \bar{D}^0$ ($\Sigma_c^+ \bar{D}^{*0}$) threshold is within the extent of the $P_c(4312)^+$ ($P_c(4457)^+$) peak, and therefore virtual [35] rather than bound states are among the plausible explanations. In simple tightly bound pentaquark models, the proximity of these states to baryon-meson thresholds would be coincidental, and furthermore, it is difficult to accommodate their narrow widths [36]. A potential barrier between diquarks, which could separate the c and \bar{c} quarks, has been proposed to solve similar difficulties for tetraquark candidates [37]. An interplay between tightly bound pentaquarks and the $\Sigma_c \bar{D}$, $\Sigma_c \bar{D}^*$ thresholds may also be responsible for the P_c^+ peaks [38–41]. Therefore, such alternative explanations cannot be ruled out. Proper identification of the internal structure of the observed states will require more experimental and theoretical scrutiny.

Acknowledgements

We express our gratitude to our colleagues in the CERN accelerator departments for the excellent performance of the LHC. We thank the technical and administrative staff at the LHCb institutes. We acknowledge support from CERN and from the national agencies: CAPES, CNPq, FAPERJ and FINEP (Brazil); MOST and NSFC (China); CNRS/IN2P3 (France); BMBF, DFG and MPG (Germany); INFN (Italy); NWO (Netherlands); MNiSW and NCN (Poland); MEN/IFA (Romania); MSHE (Russia); MinECo (Spain); SNSF and SER (Switzerland); NASU (Ukraine); STFC (United Kingdom); NSF (USA). We acknowledge the computing resources that are provided by CERN, IN2P3 (France), KIT and DESY (Germany), INFN (Italy), SURF (Netherlands), PIC (Spain), GridPP (United Kingdom), RRCKI and Yandex LLC (Russia), CSCS (Switzerland), IFIN-HH (Romania), CBPF (Brazil), PL-GRID (Poland) and OSC (USA). We are indebted to the communities behind the multiple open-source software packages on which we depend. Individual groups or members have received support from AvH Foundation (Germany); EPLANET, Marie Skłodowska-Curie Actions and ERC (European Union); ANR, Labex P2IO and OCEVU, and Région Auvergne-Rhône-Alpes (France); Key Research Program of Frontier Sciences of CAS, CAS PIFI, and the Thousand Talents Program (China); RFBR, RSF and Yandex LLC (Russia); GVA, XuntaGal and GENCAT (Spain); the Royal Society and the Leverhulme Trust (United Kingdom); Laboratory Directed Research and Development program of LANL (USA); CONACYT (Mexico).

Observation of a narrow pentaquark state, $P_c(4312)^+$, and of two-peak structure of the $P_c(4450)^+$

Supplemental Material

1 $\Lambda_b^0 \rightarrow J/\psi p K^-$ candidates

The $\Lambda_b^0 \rightarrow J/\psi p K^-$ sample analyzed in the Letter is selected by requiring that the invariant mass of $J/\psi p K^-$ candidates is in the 5605–5635 MeV range. To determine the Λ_b^0 signal yield within this range, the background density is linearly interpolated from the 5480–5580 MeV and 5660–5760 MeV sidebands to the signal region, as illustrated in Fig. S1. There are 246k Λ_b^0 decays with 6.4% background contamination in the analyzed sample.

After selecting candidates in the Λ_b^0 signal region indicated in Fig. S1, the Λ_b^0 mass constraint is imposed on all Λ_b^0 candidates, in addition to the J/ψ mass and vertex constraints, to improve the $m_{J/\psi p}$ resolution. To a good approximation, the mass resolution

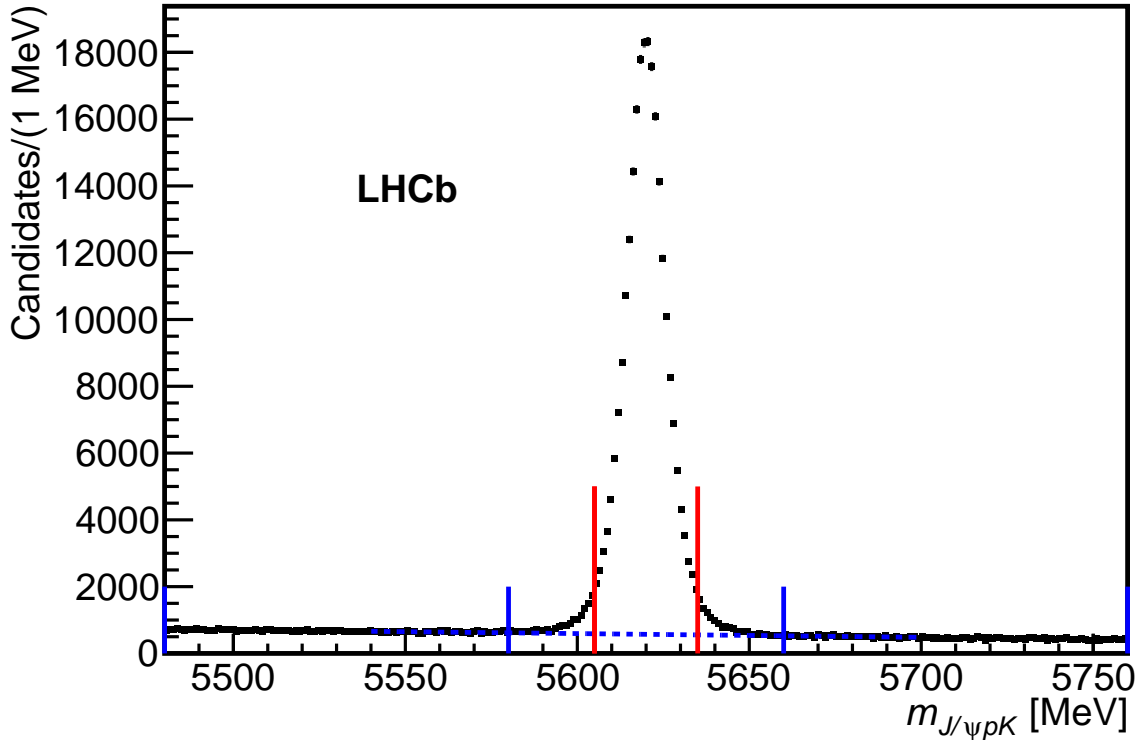


Figure S1: Invariant mass spectrum of $J/\psi p K^-$ candidates. The Λ_b^0 signal region is between the vertical red lines. A linear interpolation of the background, determined from the sideband regions (bounded by the shorter vertical blue lines), to the signal region is shown by the dashed blue line.

is Gaussian with a standard deviation (σ_m) given by

$$\sigma_m(m_{J/\psi p}) = [2.71 - 6.56 \cdot 10^{-6}(m_{J/\psi p}/\text{MeV} - 4567)^2] \text{ MeV}. \quad (\text{S1})$$

2 Example fit with interference

Figure S2 shows an example fit with interfering resonances.

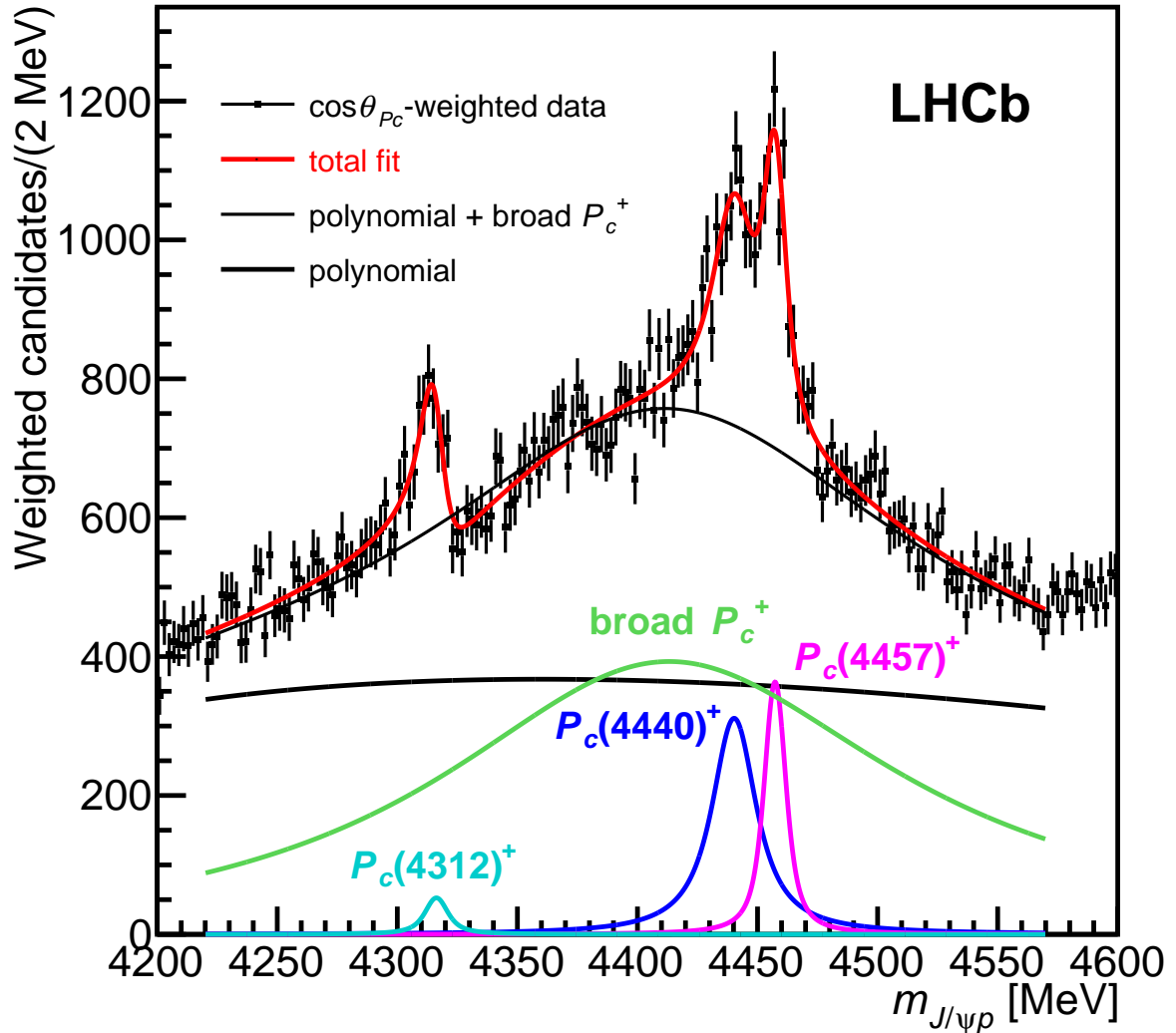


Figure S2: Fit to the $\cos\theta_{P_c}$ -weighted $m_{J/\psi p}$ distribution with four BW amplitudes and a linear background. The broad P_c^+ state is added coherently to the $P_c(4312)^+$ amplitude. In this fit model, the magnitude of the $P_c(4312)^+$ peak in the data is dominated by its interference with the broad P_c^+ state. Each P_c^+ contribution is displayed as the BW amplitude squared (the interference contributions are not shown individually).

3 Study of triangle diagrams

The narrow widths of the P_c^+ peaks make a compelling case for the bound-state character of the observed states. However, it has been pointed out by many authors [16–19] that peaking structures in this $J/\psi p$ mass range can also be generated by triangle diagrams (see Fig. S3). In these processes, the Λ_b^0 baryon (of mass m_1) decays into two nearly on-mass-shell hadrons, one of which (of mass $m_h \equiv \sqrt{t}$) is an excited strange meson or baryon (denoted here as h) that subsequently emits a kaon (of mass m_2) and a non-strange decay product (of mass m_4) that rescatters with the other Λ_b^0 child (of mass m_3) into the $J/\psi p$ system (of $m_{J/\psi p} \equiv \sqrt{s}$). Such triangle-diagram processes are known to peak when all three hadrons in the triangle are nearly on their mass shells. Since the overall probability across coupled channels must be conserved, a peak in the $J/\psi p$ channel is only possible if there is a corresponding depletion in the final state composed of the particles that rescatter in Fig. S3 to form the $J/\psi p$ [42].

The triangle-diagram contribution often peaks at a threshold, given by the sum of the masses of the rescattering hadrons ($m_3 + m_4$) creating a cusp. For a fine-tuned BW resonance mass of the intermediate hadron h (M_0), the rate can peak above (but never below) the corresponding threshold. The amplitude for a triangle-diagram process, which incorporates a finite width for the exchanged particle (Γ_0), is given by

$$A(s) \propto \int_{(m_2+m_4)^2}^{\infty} dt |\text{BW}(t|M_0, \Gamma_0)|^2 F(t, s), \quad (\text{S2})$$

where all quantities are defined in Fig. S3. The BW term corresponds to the exchanged h hadron. The Feynman triangle-amplitude formula is expressed in terms of a one-dimensional integral over a single Feynman parameter x as follows:

$$F(t, s) \equiv 2 \int_0^1 \frac{dx}{y_- - y_+} \left[\log \left(1 - \frac{2sx}{y_+} \right) - \log \left(1 - \frac{2sx}{y_-} \right) \right], \quad (\text{S3})$$

where

$$\begin{aligned} y_{\pm} \equiv y_{\pm}(s, t, x) \equiv & (m_1^2 - m_2^2 + s)x - m_1^2 + m_2^2 + m_3^2 - m_4^2 \\ & \pm \{ i\epsilon + x^2 \lambda(s, m_1^2, m_2^2) + 2x [(m_1^2 + m_2^2 - m_3^2 - m_4^2 + 2t)s \\ & - (m_1^2 - m_2^2)(m_1^2 - m_2^2 - m_3^2 + m_4^2)] - 4st + (m_1^2 - m_2^2 - m_3^2 + m_4^2)^2 \}^{1/2}. \end{aligned} \quad (\text{S4})$$

Here, $\lambda(a, b, c) = a^2 + b^2 + c^2 - 2ab - 2ac - 2bc$ and ϵ is a small real number.

The 4457 MeV structure peaks near the $\Lambda_c^+(2595)\bar{D}^0$ threshold ($J^P = 1/2^+$) [18]. The best h candidate for the corresponding triangle diagram is the $D_{s1}(2860)^-$ meson, which has a mass of 2859 ± 27 MeV and a width of 159 ± 80 MeV [25]. The $P_c(4312)^+$ is not far from the $\Lambda_c^+\bar{D}^{*0}$ threshold ($J^P = 1/2^-$ or $3/2^-$). Exchanging an excited $1^- D_s^{**}$ meson with $M_0 = 3288$ MeV produces the peak at 4312 MeV in the narrow width approximation ($\Gamma_0 \rightarrow 0$). The $P_c(4440)^+$ is well above the $\chi_{c0}p$ threshold ($1/2^+$). Exchanging an excited $1/2^+ \Lambda^*$ with $M_0 = 2153$ MeV produces a peak at the right mass when $\Gamma_0 \rightarrow 0$. In fact, a good quality fit to all three P_c^+ peaks is obtained when Γ_0 is small, as illustrated in Fig. S4 (top). However, this interpretation is unrealistic for the $P_c(4312)^+$ and $P_c(4440)^+$ peaks. When more plausible widths for the excited hadrons are used, such as $\Gamma_0 = 50$ MeV, no narrow peaks can be created above the thresholds, as shown in Fig. S4 (bottom).

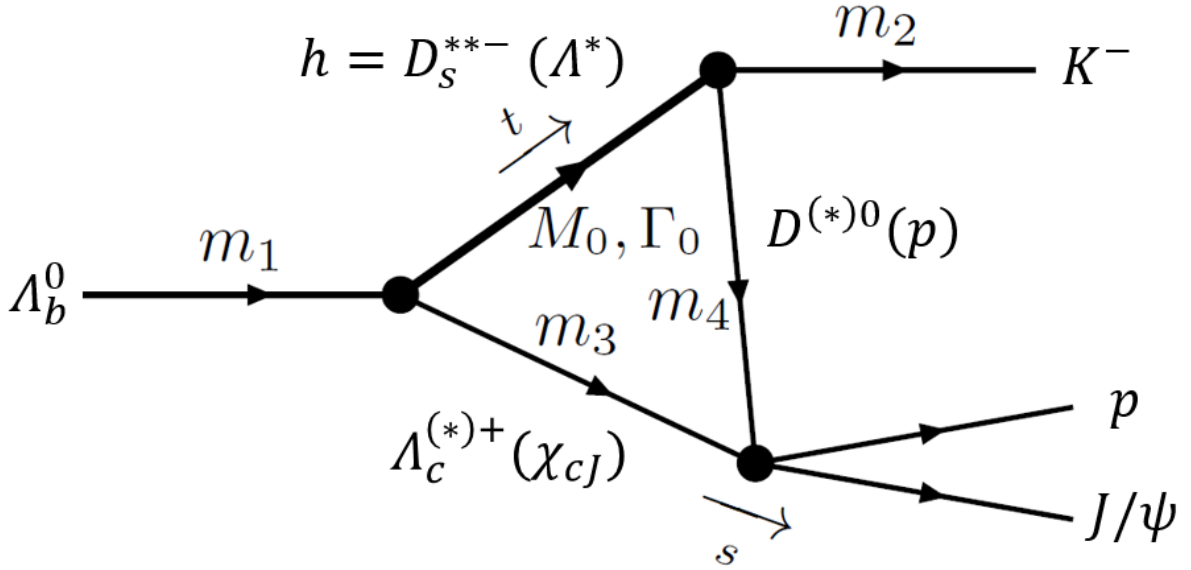


Figure S3: Triangle diagram for the $\Lambda_b^0 \rightarrow J/\psi p K^-$ decay. The figure defines the symbols used in the formulae in the text.

The triangle-diagram hypothesis is more plausible for the $P_c(4457)^+$ state. An example fit using two BW terms and one triangle-diagram amplitude is shown in Fig. S5. The fit quality is lower than that obtained using three BW amplitudes. However, further investigation of this interpretation of the $P_c(4457)^+$ state is warranted within an amplitude analysis, which will provide greater discrimination between the triangle-diagram and BW amplitudes.

4 Comments on the results in Ref. [1]

The $P_c(4450)^+$ state reported in Ref. [1] should be considered obsolete and replaced by the $P_c(4440)^+$ and $P_c(4457)^+$ states. The six-dimensional amplitude analysis reported in Ref. [1], which provided evidence for the $P_c(4380)^+$ state, is also obsolete since it used the single $P_c(4450)^+$ state and it lacked the $P_c(4312)^+$ state. Therefore, the results presented in the Letter weaken the previously reported evidence for the $P_c(4380)^+$ state, but do not contradict its existence, since the present one-dimensional analysis is not sensitive to wide P_c^+ states. Only a future six-dimensional amplitude analysis of $\Lambda_b^0 \rightarrow J/\psi p K^-$ decays that includes the $P_c(4440)^+$, $P_c(4457)^+$, and $P_c(4312)^+$ states will be able to determine if there is still evidence for the $P_c(4380)^+$ state or any other wide P_c^+ states.

Reference [1] performed a cross-check of the six-dimensional amplitude model by replacing the BW function for the $P_c(4450)^+$ state, under the preferred quantum-number assignment, by complex amplitudes in six narrow $m_{J/\psi p}$ bins near the peak region. The complex amplitudes obtained from this cross-check had large statistical uncertainties. The systematic uncertainties were not evaluated. This cross-check was repeated for the $P_c(4380)^+$ state. The results of both cross-checks were displayed as Argand diagrams, which were consistent with the expected phase motion from the BW functions (more so for the $P_c(4450)^+$ structure than for the $P_c(4380)^+$), but that should now be considered

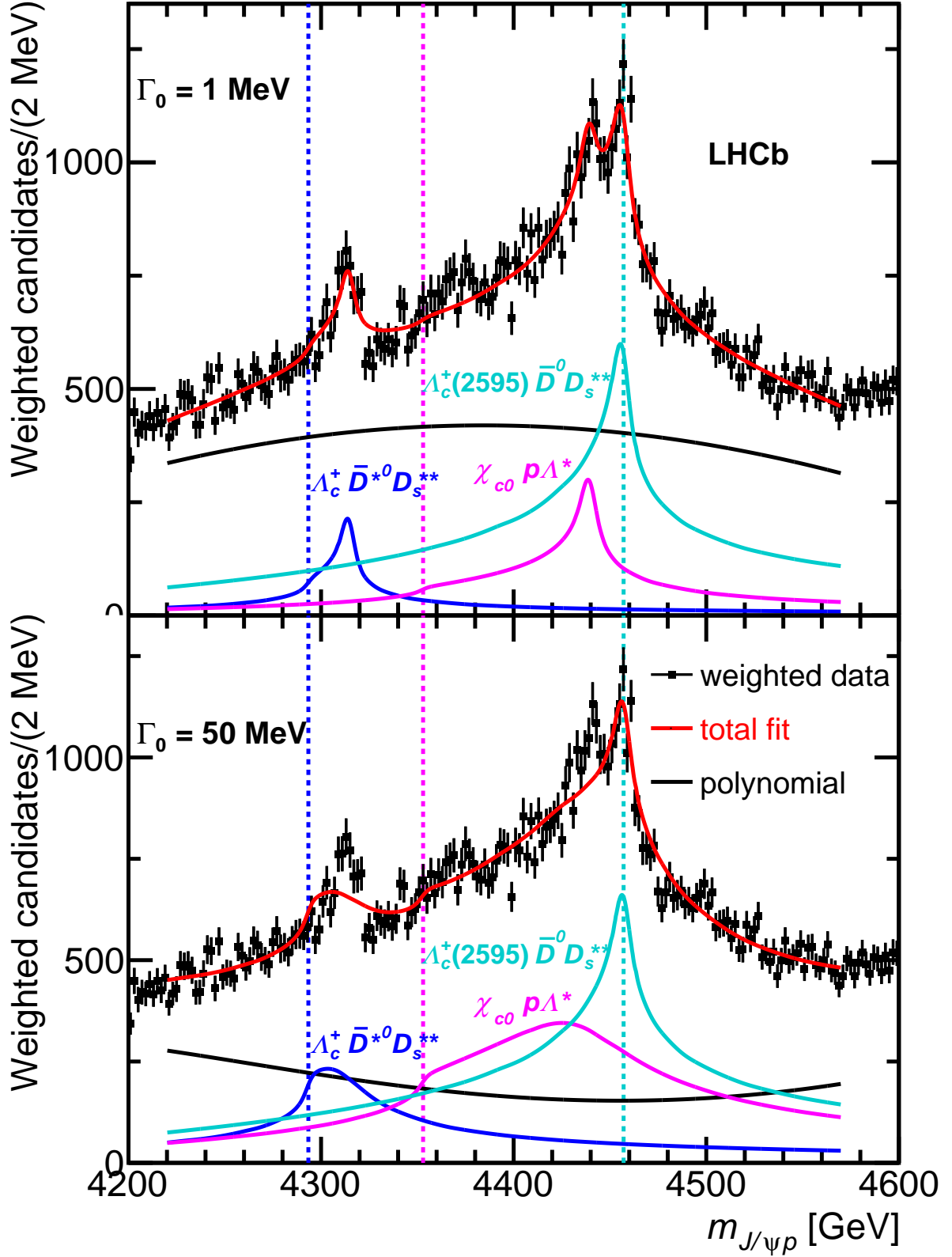


Figure S4: Fit of three triangle-diagram amplitudes and a quadratic background to the $\cos \theta_{Pc^-}$ -weighted distribution. The widths of the excited particles exchanged in the triangles is (top) an unrealistic value of 1 MeV or (bottom) a more plausible value of 50 MeV. Individual triangle diagram contributions are also shown. The dashed vertical lines are the $\Lambda_c^+ \bar{D}^{*0}$, $\chi_{c0} p$ and $\Lambda_c^+(2595) \bar{D}^0$ thresholds.

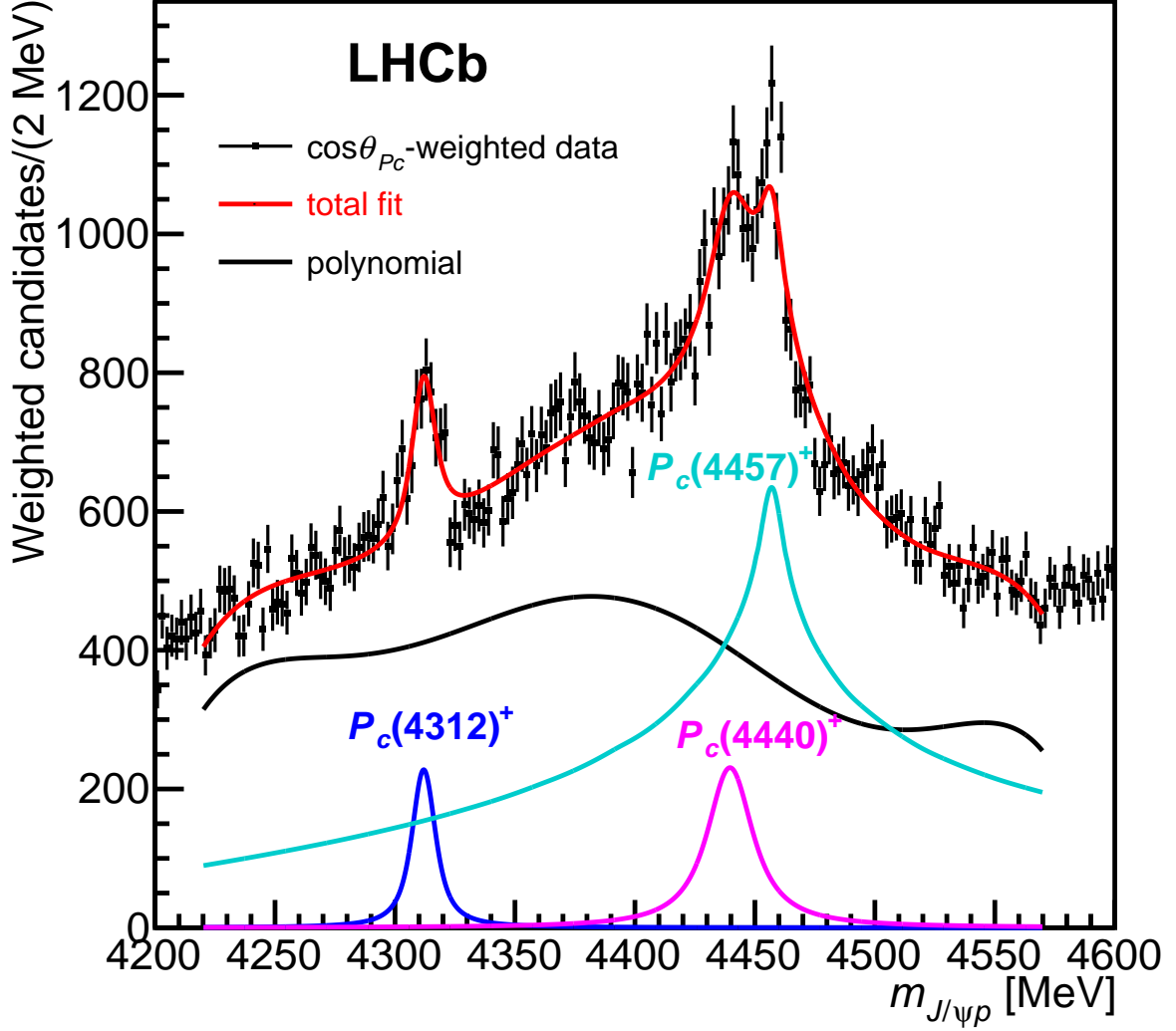


Figure S5: Fit of two BW amplitudes, one triangle-diagram amplitude, and a sixth-order polynomial background to the $\cos \theta_{P_c}$ -weighted distribution. The width of the excited D_s^* state exchanged in the triangle loop is set to $\Gamma(D_{s1}(2860)^-) = 159$ MeV [25, 43]. The predicted width for this D_s^* state, interpreted as the 1^3D_1 $s\bar{c}$ excitation in the quark model, is 197 MeV [44].

obsolete. The $P_c(4380)^+$ Argand diagram was obtained using a model in which the $P_c(4450)^+$ structure was represented by only one resonance and the $P_c(4312)^+$ state was not included. The $P_c(4450)^+$ Argand diagram was obtained using a model in which the $P_c(4312)^+$ state was missing, and under the assumption that only a single partial wave describes the structure peaking at 4450 MeV. This assumption is difficult to justify given the two-peak observation presented in the Letter. Furthermore, since the natural widths of the $P_c(4440)^+$ and $P_c(4457)^+$ states are comparable to the mass resolution, the $P_c(4450)^+$ Argand diagram reported in Ref. [1] would need to have the mass-resolution effects unfolded to probe the underlying complex phase motion even if both states happened to have the same quantum numbers.

References

- [1] LHCb collaboration, R. Aaij *et al.*, *Observation of $J/\psi p$ resonances consistent with pentaquark states in $\Lambda_b^0 \rightarrow J/\psi p K^-$ decays*, Phys. Rev. Lett. **115** (2015) 072001, arXiv:1507.03414.
- [2] LHCb collaboration, R. Aaij *et al.*, *Model-independent evidence for $J/\psi p$ contributions to $\Lambda_b^0 \rightarrow J/\psi p K^-$ decays*, Phys. Rev. Lett. **117** (2016) 082002, arXiv:1604.05708.
- [3] L. Maiani, A. D. Polosa, and V. Riquer, *The new pentaquarks in the diquark model*, Phys. Lett. **B749** (2015) 289, arXiv:1507.04980.
- [4] R. F. Lebed, *The pentaquark candidates in the dynamical diquark picture*, Phys. Lett. **B749** (2015) 454, arXiv:1507.05867.
- [5] V. V. Anisovich *et al.*, *Pentaquarks and resonances in the pJ/ψ spectrum*, arXiv:1507.07652.
- [6] G.-N. Li, X.-G. He, and M. He, *Some predictions of diquark model for hidden charm pentaquark discovered at the LHCb*, JHEP **12** (2015) 128, arXiv:1507.08252.
- [7] R. Ghosh, A. Bhattacharya, and B. Chakrabarti, *A study on $P_c^*(4380)$ and $P_c^*(4450)$ in the quasi particle diquark model*, Phys. Part. Nucl. Lett. **14** (2017) 550, arXiv:1508.00356.
- [8] Z.-G. Wang, *Analysis of $P_c(4380)$ and $P_c(4450)$ as pentaquark states in the diquark model with QCD sum rules*, Eur. Phys. J. **C76** (2016) 70, arXiv:1508.01468.
- [9] R. Zhu and C.-F. Qiao, *Pentaquark states in a diquark-triquark model*, Phys. Lett. **B756** (2016) 259, arXiv:1510.08693.
- [10] M. Karliner and J. L. Rosner, *New exotic meson and baryon resonances from doubly-heavy hadronic molecules*, Phys. Rev. Lett. **115** (2015) 122001, arXiv:1506.06386.
- [11] R. Chen, X. Liu, X.-Q. Li, and S.-L. Zhu, *Identifying exotic hidden-charm pentaquarks*, Phys. Rev. Lett. **115** (2015) 132002, arXiv:1507.03704.
- [12] H.-X. Chen *et al.*, *Towards exotic hidden-charm pentaquarks in QCD*, Phys. Rev. Lett. **115** (2015) 172001, arXiv:1507.03717.
- [13] L. Roca, J. Nieves, and E. Oset, *LHCb pentaquark as a $\bar{D}^* \Sigma_c - \bar{D}^* \Sigma_c^*$ molecular state*, Phys. Rev. **D92** (2015) 094003, arXiv:1507.04249.
- [14] J. He, *$\bar{D} \Sigma_c^*$ and $\bar{D}^* \Sigma_c$ interactions and the LHCb hidden-charmed pentaquarks*, Phys. Lett. **B753** (2016) 547, arXiv:1507.05200.
- [15] H. Huang, C. Deng, J. Ping, and F. Wang, *Possible pentaquarks with heavy quarks*, Eur. Phys. J. **C76** (2016) 624, arXiv:1510.04648.
- [16] F.-K. Guo, U.-G. Meißner, W. Wang, and Z. Yang, *How to reveal the exotic nature of the $P_c(4450)$* , Phys. Rev. **D92** (2015) 071502, arXiv:1507.04950.

- [17] U.-G. Meißner and J. A. Oller, *Testing the χ_{c1p} composite nature of the $P_c(4450)$* , Phys. Lett. **B751** (2015) 59, arXiv:1507.07478.
- [18] X.-H. Liu, Q. Wang, and Q. Zhao, *Understanding the newly observed heavy pentaquark candidates*, Phys. Lett. **B757** (2016) 231, arXiv:1507.05359.
- [19] M. Mikhasenko, *A triangle singularity and the LHCb pentaquarks*, arXiv:1507.06552.
- [20] LHCb collaboration, A. A. Alves Jr. *et al.*, *The LHCb detector at the LHC*, JINST **3** (2008) S08005.
- [21] LHCb collaboration, R. Aaij *et al.*, *LHCb detector performance*, Int. J. Mod. Phys. **A30** (2015) 1530022, arXiv:1412.6352.
- [22] S. Capstick and N. Isgur, *Baryons in a relativized quark model with chromodynamics*, Phys. Rev. **D34** (1986) 2809.
- [23] U. Loring, B. C. Metsch, and H. R. Petry, *The light-baryon spectrum in a relativistic quark model with instanton induced quark forces: the strange baryon spectrum*, Eur. Phys. J. **A10** (2001) 447, arXiv:hep-ph/0103290.
- [24] C. Fernandez-Ramirez *et al.*, *Coupled-channel model for $\bar{K}N$ scattering in the resonant region*, Phys. Rev. **D93** (2016) 034029, arXiv:1510.07065.
- [25] Particle Data Group, M. Tanabashi *et al.*, *Review of particle physics*, Phys. Rev. **D98** (2018) 030001.
- [26] LHCb collaboration, R. Aaij *et al.*, *Search for structure in the $B_s^0\pi^\pm$ invariant mass spectrum*, Phys. Rev. Lett. **117** (2016) 152003, arXiv:1608.00435.
- [27] See Supplemental Material to this Letter, which includes Refs. [42–44].
- [28] T. J. Burns, *Phenomenology of $P_c(4380)^+$, $P_c(4450)^+$ and related states*, Eur. Phys. J. **A51** (2015) 152, arXiv:1509.02460.
- [29] W. L. Wang, F. Huang, Z. Y. Zhang, and B. S. Zou, *$\Sigma_c\bar{D}$ and $\Lambda_c^+\bar{D}$ states in a chiral quark model*, Phys. Rev. **C84** (2011) 015203, arXiv:1101.0453.
- [30] Z.-C. Yang *et al.*, *Possible hidden-charm molecular baryons composed of anti-charmed meson and charmed baryon*, Chin. Phys. **C36** (2012) 6, arXiv:1105.2901.
- [31] J.-J. Wu, T.-S. H. Lee, and B. S. Zou, *Nucleon resonances with hidden charm in coupled-channel models*, Phys. Rev. **C85** (2012) 044002, arXiv:1202.1036.
- [32] J.-J. Wu, R. Molina, E. Oset, and B. S. Zou, *Prediction of narrow N^* and Λ^* resonances with hidden charm above 4 GeV*, Phys. Rev. Lett. **105** (2010) 232001, arXiv:1007.0573.
- [33] J.-J. Wu, R. Molina, E. Oset, and B. S. Zou, *Dynamically generated N^* and Λ^* resonances in the hidden charm sector around 4.3 GeV*, Phys. Rev. **C84** (2011) 015202, arXiv:1011.2399.

- [34] C. W. Xiao, J. Nieves, and E. Oset, *Combining heavy quark spin and local hidden gauge symmetries in the dynamical generation of hidden charm baryons*, Phys. Rev. **D88** (2013) 056012, arXiv:1304.5368.
- [35] W. R. Frazer and A. W. Hendry, *S-matrix poles close to threshold*, Phys. Rev. **134** (1964) B1307.
- [36] E. Hiyama, A. Hosaka, M. Oka, and J.-M. Richard, *Quark model estimate of hidden-charm pentaquark resonances*, Phys. Rev. **C98** (2018) 045208, arXiv:1803.11369.
- [37] L. Maiani, A. D. Polosa, and V. Riquer, *A theory of X and Z multiquark resonances*, Phys. Lett. **B778** (2018) 247, arXiv:1712.05296.
- [38] D. V. Bugg, *How resonances can synchronise with thresholds*, J. Phys. **G35** (2008) 075005, arXiv:0802.0934.
- [39] F.-K. Guo, C. Hanhart, Q. Wang, and Q. Zhao, *Could the near-threshold XYZ states be simply kinematic effects?*, Phys. Rev. **D91** (2015) 051504, arXiv:1411.5584.
- [40] S. H. Blitz and R. F. Lebed, *Tetraquark cusp effects from diquark pair production*, Phys. Rev. **D91** (2015) 094025, arXiv:1503.04802.
- [41] F.-K. Guo *et al.*, *Interplay of quark and meson degrees of freedom in near-threshold states: A practical parametrization for line shapes*, Phys. Rev. **D93** (2016) 074031, arXiv:1602.00940.
- [42] A. P. Szczepaniak, *Dalitz plot distributions in presence of triangle singularities*, Phys. Lett. **B757** (2016) 61, arXiv:1510.01789.
- [43] LHCb collaboration, R. Aaij *et al.*, *Observation of overlapping spin-1 and spin-3 $\bar{D}^0 K^-$ resonances at mass 2.86 GeV/c²*, Phys. Rev. Lett. **113** (2014) 162001, arXiv:1407.7574.
- [44] S. Godfrey and K. Moats, *Properties of excited charm and charm-strange mesons*, Phys. Rev. **D93** (2016) 034035, arXiv:1510.08305.

LHCb collaboration

R. Aaij²⁸, C. Abellán Beteta⁴⁶, B. Adeva⁴³, M. Adinolfi⁵⁰, C.A. Aidala⁸⁰, Z. Ajaltouni⁶, S. Akar⁶¹, P. Albicocco¹⁹, J. Albrecht¹¹, F. Alessio⁴⁴, M. Alexander⁵⁵, A. Alfonso Alberio⁴², G. Alkhazov⁴¹, P. Alvarez Cartelle⁵⁷, A.A. Alves Jr⁴³, S. Amato², Y. Amhis⁸, L. An¹⁸, L. Anderlini¹⁸, G. Andreassi⁴⁵, M. Andreotti¹⁷, J.E. Andrews⁶², F. Archilli¹⁹, P. d'Argent¹³, J. Arnau Romeu⁷, A. Artamonov⁴⁰, M. Artuso⁶³, K. Arzymatov³⁷, E. Aslanides⁷, M. Atzeni⁴⁶, B. Audurier²³, S. Bachmann¹³, J.J. Back⁵², S. Baker⁵⁷, V. Balagura^{8,b}, W. Baldini^{17,44}, A. Baranov³⁷, R.J. Barlow⁵⁸, S. Barsuk⁸, W. Barter⁵⁷, M. Bartolini²⁰, F. Baryshnikov⁷⁶, V. Batozskaya³², B. Batsukh⁶³, A. Battig¹¹, V. Battista⁴⁵, A. Bay⁴⁵, F. Bedeschi²⁵, I. Bediaga¹, A. Beiter⁶³, L.J. Bel²⁸, V. Belavin³⁷, S. Belin²³, N. Bely⁶⁶, V. Bellec⁴⁵, N. Belloli^{21,i}, K. Belous⁴⁰, I. Belyaev³⁴, E. Ben-Haim⁹, G. Bencivenni¹⁹, S. Benson²⁸, S. Beranek¹⁰, A. Berezhnoy³⁵, R. Bernet⁴⁶, D. Berninghoff¹³, E. Bertholet⁹, A. Bertolin²⁴, C. Betancourt⁴⁶, F. Betti^{16,e}, M.O. Bettler⁵¹, M. van Beuzekom²⁸, I.a. Bezshyiko⁴⁶, S. Bhasin⁵⁰, J. Bhom³⁰, M.S. Bieker¹¹, S. Bifani⁴⁹, P. Billoir⁹, A. Birnkraut¹¹, A. Bizzeti^{18,u}, M. Bjørn⁵⁹, M.P. Blago⁴⁴, T. Blake⁵², F. Blanc⁴⁵, S. Blusk⁶³, D. Bobulska⁵⁵, V. Bocci²⁷, O. Boente Garcia⁴³, T. Boettcher⁶⁰, A. Bondar^{39,x}, N. Bondar⁴¹, S. Borghi^{58,44}, M. Borisyak³⁷, M. Borsato¹³, M. Boubdir¹⁰, T.J.V. Bowcock⁵⁶, C. Bozzi^{17,44}, S. Braun¹³, A. Brea Rodriguez⁴³, M. Brodski⁴⁴, J. Brodzicka³⁰, A. Brossa Gonzalo⁵², D. Brundu^{23,44}, E. Buchanan⁵⁰, A. Buonaura⁴⁶, C. Burr⁵⁸, A. Bursche²³, J.S. Butter²⁸, J. Buytaert⁴⁴, W. Byczynski⁴⁴, S. Cadeddu²³, H. Cai⁶⁸, R. Calabrese^{17,g}, S. Cali¹⁹, R. Calladine⁴⁹, M. Calvi^{21,i}, M. Calvo Gomez^{42,m}, A. Camboni^{42,m}, P. Campana¹⁹, D.H. Campora Perez⁴⁴, L. Capriotti^{16,e}, A. Carbone^{16,e}, G. Carboni²⁶, R. Cardinale²⁰, A. Cardini²³, P. Carniti^{21,i}, K. Carvalho Akiba², A. Casais Vidal⁴³, G. Casse⁵⁶, M. Cattaneo⁴⁴, G. Cavallero²⁰, R. Cenci^{25,p}, M.G. Chapman⁵⁰, M. Charles^{9,44}, Ph. Charpentier⁴⁴, G. Chatzikonstantinidis⁴⁹, M. Chefdeville⁵, V. Chekalina³⁷, C. Chen³, S. Chen²³, S.-G. Chitic⁴⁴, V. Chobanova⁴³, M. Chrzaszcz⁴⁴, A. Chubykin⁴¹, P. Ciambrone¹⁹, X. Cid Vidal⁴³, G. Ciezarek⁴⁴, F. Cindolo¹⁶, P.E.L. Clarke⁵⁴, M. Clemencic⁴⁴, H.V. Cliff⁵¹, J. Closier⁴⁴, V. Coco⁴⁴, J.A.B. Coelho⁸, J. Cogan⁷, E. Cogneras⁶, L. Cojocariu³³, P. Collins⁴⁴, T. Colombo⁴⁴, A. Comerma-Montells¹³, A. Contu²³, G. Coombs⁴⁴, S. Coquereau⁴², G. Corti⁴⁴, C.M. Costa Sobral⁵², B. Couturier⁴⁴, G.A. Cowan⁵⁴, D.C. Craik⁶⁰, A. Crocombe⁵², M. Cruz Torres¹, R. Currie⁵⁴, C. D'Ambrosio⁴⁴, C.L. Da Silva⁸², E. Dall'Occo²⁸, J. Dalseno^{43,v}, A. Danilina³⁴, A. Davis⁵⁸, O. De Aguiar Francisco⁴⁴, K. De Bruyn⁴⁴, S. De Capua⁵⁸, M. De Cian⁴⁵, J.M. De Miranda¹, L. De Paula², M. De Serio^{15,d}, P. De Simone¹⁹, C.T. Dean⁵⁵, W. Dean⁸⁰, D. Decamp⁵, L. Del Buono⁹, B. Delaney⁵¹, H.-P. Dembinski¹², M. Demmer¹¹, A. Dendek³¹, D. Derkach³⁸, O. Deschamps⁶, F. Desse⁸, F. Dettori²³, B. Dey⁶⁹, A. Di Canto⁴⁴, P. Di Nezza¹⁹, S. Didenko⁷⁶, H. Dijkstra⁴⁴, F. Dordei²³, M. Dorigo^{25,y}, A. Dosil Suárez⁴³, L. Douglas⁵⁵, A. Dovbnya⁴⁷, K. Dreimanis⁵⁶, L. Dufour⁴⁴, G. Dujany⁹, P. Durante⁴⁴, J.M. Durham⁸², D. Dutta⁵⁸, R. Dzhelyadin^{40,†}, M. Dziewiecki¹³, A. Dziurda³⁰, A. Dzyuba⁴¹, S. Easo⁵³, U. Egede⁵⁷, V. Egorychev³⁴, S. Eidelman^{39,x}, S. Eisenhardt⁵⁴, U. Eitschberger¹¹, S. Ek-In⁴⁵, R. Ekelhof¹¹, L. Eklund⁵⁵, S. Ely⁶³, A. Ene³³, S. Escher¹⁰, S. Esen²⁸, T. Evans⁶¹, A. Falabella¹⁶, N. Farley⁴⁹, S. Farry⁵⁶, D. Fazzini⁸, P. Fernandez Declara⁴⁴, A. Fernandez Prieto⁴³, C. Fernández-Ramírez⁷³, F. Ferrari^{16,e}, L. Ferreira Lopes⁴⁵, F. Ferreira Rodrigues², S. Ferreres Sole²⁸, M. Ferro-Luzzi⁴⁴, S. Filippov³⁶, R.A. Fini¹⁵, M. Fiorini^{17,g}, M. Firlej³¹, C. Fitzpatrick⁴⁴, T. Fiutowski³¹, F. Fleuret^{8,b}, M. Fontana⁴⁴, F. Fontanelli^{20,h}, R. Forty⁴⁴, V. Franco Lima⁵⁶, M. Franco Sevilla⁶², M. Frank⁴⁴, C. Frei⁴⁴, J. Fu^{22,q}, W. Funk⁴⁴, C. Färber⁴⁴, M. Féo⁴⁴, E. Gabriel⁵⁴, A. Gallas Torreira⁴³, D. Galli^{16,e}, S. Gallorini²⁴, S. Gambetta⁵⁴, Y. Gan³, M. Gandelman², P. Gandini²², Y. Gao³, L.M. Garcia Martin⁷⁸, B. Garcia Plana⁴³, J. García Pardiñas⁴⁶, J. Garra Tico⁵¹, L. Garrido⁴², D. Gascon⁴², C. Gaspar⁴⁴, G. Gazzoni⁶, D. Gerick¹³, E. Gersabeck⁵⁸, M. Gersabeck⁵⁸, T. Gershon⁵², D. Gerstel⁷, Ph. Ghez⁵, V. Gibson⁵¹, O.G. Girard⁴⁵, P. Gironella Gironell⁴²,

L. Giubega³³, K. Gizdov⁵⁴, V.V. Gligorov⁹, D. Golubkov³⁴, A. Golutvin^{57,76}, A. Gomes^{1,a},
 I.V. Gorelov³⁵, C. Gotti^{21,i}, E. Govorkova²⁸, J.P. Grabowski¹³, R. Graciani Diaz⁴²,
 L.A. Granado Cardoso⁴⁴, E. Graugés⁴², E. Graverini⁴⁵, G. Graziani¹⁸, A. Grecu³³, R. Greim²⁸,
 P. Griffith²³, L. Grillo⁵⁸, L. Gruber⁴⁴, B.R. Gruberg Cazon⁵⁹, C. Gu³, X. Guo⁶⁷, E. Gushchin³⁶,
 A. Guth¹⁰, Yu. Guz^{40,44}, T. Gys⁴⁴, C. Göbel⁶⁵, T. Hadavizadeh⁵⁹, C. Hadjivasiliou⁶,
 G. Haefeli⁴⁵, C. Haen⁴⁴, S.C. Haines⁵¹, B. Hamilton⁶², Q. Han⁶⁹, X. Han¹³, T.H. Hancock⁵⁹,
 S. Hansmann-Menzemer¹³, N. Harnew⁵⁹, T. Harrison⁵⁶, C. Hasse⁴⁴, M. Hatch⁴⁴, J. He⁶⁶,
 M. Hecker⁵⁷, K. Heinicke¹¹, A. Heister¹¹, K. Hennessy⁵⁶, L. Henry⁷⁸, E. van Herwijnen⁴⁴,
 J. Heuel¹⁰, M. Heß⁷¹, A. Hicheur⁶⁴, R. Hidalgo Charman⁵⁸, D. Hill⁵⁹, M. Hilton⁵⁸,
 P.H. Hopchev⁴⁵, J. Hu¹³, W. Hu⁶⁹, W. Huang⁶⁶, Z.C. Huard⁶¹, W. Hulsbergen²⁸, T. Humair⁵⁷,
 M. Hushchyn³⁸, D. Hutchcroft⁵⁶, D. Hynds²⁸, P. Ibis¹¹, M. Idzik³¹, P. Ilten⁴⁹, A. Inglessi⁴¹,
 A. Inyakin⁴⁰, K. Ivshin⁴¹, R. Jacobsson⁴⁴, S. Jakobsen⁴⁴, J. Jalocha⁵⁹, E. Jans²⁸, B.K. Jashal⁷⁸,
 A. Jawahery⁶², F. Jiang³, M. John⁵⁹, D. Johnson⁴⁴, C.R. Jones⁵¹, C. Joram⁴⁴, B. Jost⁴⁴,
 N. Jurik⁵⁹, S. Kandybei⁴⁷, M. Karacson⁴⁴, J.M. Kariuki⁵⁰, S. Karodia⁵⁵, N. Kazeev³⁸,
 M. Kecke¹³, F. Keizer⁵¹, M. Kelsey⁶³, M. Kenzie⁵¹, T. Ketel²⁹, B. Khanji⁴⁴, A. Kharisova⁷⁷,
 C. Khurewathanakul⁴⁵, K.E. Kim⁶³, T. Kirn¹⁰, V.S. Kirsebom⁴⁵, S. Klaver¹⁹,
 K. Klimaszewski³², S. Koliiev⁴⁸, M. Kolpin¹³, A. Kondybayeva⁷⁶, A. Konoplyannikov³⁴,
 R. Kopecna¹³, P. Koppenburg²⁸, I. Kostiuk^{28,48}, O. Kot⁴⁸, S. Kotriakhova⁴¹, M. Kozeiha⁶,
 L. Kravchuk³⁶, M. Kreps⁵², F. Kress⁵⁷, S. Kretzschmar¹⁰, P. Krokovny^{39,x}, W. Krupa³¹,
 W. Krzemien³², W. Kucewicz^{30,l}, M. Kucharczyk³⁰, V. Kudryavtsev^{39,x}, G.J. Kunde⁸²,
 A.K. Kuonen⁴⁵, T. Kvaratskheliya³⁴, D. Lacarrere⁴⁴, G. Lafferty⁵⁸, A. Lai²³, D. Lancierini⁴⁶,
 G. Lanfranchi¹⁹, C. Langenbruch¹⁰, T. Latham⁵², C. Lazzeroni⁴⁹, R. Le Gac⁷, A. Leflat³⁵,
 R. Lefèvre⁶, F. Lemaitre⁴⁴, O. Leroy⁷, T. Lesiak³⁰, B. Leverington¹³, H. Li⁶⁷, P.-R. Li^{66,ab},
 X. Li⁸², Y. Li⁴, Z. Li⁶³, X. Liang⁶³, T. Likhomanenko⁷⁵, R. Lindner⁴⁴, P. Ling⁶⁷, F. Lionetto⁴⁶,
 V. Lisovskyi⁸, G. Liu⁶⁷, X. Liu³, D. Loh⁵², A. Loi²³, J. Lomba Castro⁴³, I. Longstaff⁵⁵,
 J.H. Lopes², G. Loustau⁴⁶, G.H. Lovell⁵¹, D. Lucchesi^{24,o}, M. Lucio Martinez⁴³, Y. Luo³,
 A. Lupato²⁴, E. Luppi^{17,g}, O. Lupton⁵², A. Lusiani²⁵, X. Lyu⁶⁶, R. Ma⁶⁷, F. Machefert⁸,
 F. Maciuc³³, V. Macko⁴⁵, P. Mackowiak¹¹, S. Maddrell-Mander⁵⁰, O. Maev^{41,44}, K. Maguire⁵⁸,
 D. Maisuzenko⁴¹, M.W. Majewski³¹, S. Malde⁵⁹, B. Malecki⁴⁴, A. Malinin⁷⁵, T. Maltsev^{39,x},
 H. Malygina¹³, G. Manca^{23,f}, G. Mancinelli⁷, D. Marangotto^{22,q}, J. Maratas^{6,w},
 J.F. Marchand⁵, U. Marconi¹⁶, C. Marin Benito⁸, M. Marinangeli⁴⁵, P. Marino⁴⁵, J. Marks¹³,
 P.J. Marshall⁵⁶, G. Martellotti²⁷, L. Martinazzoli⁴⁴, M. Martinelli^{44,21}, D. Martinez Santos⁴³,
 F. Martinez Vidal⁷⁸, A. Massafferri¹, M. Materok¹⁰, R. Matev⁴⁴, A. Mathad⁴⁶, Z. Mathe⁴⁴,
 V. Matiunin³⁴, C. Matteuzzi²¹, K.R. Mattioli⁸⁰, A. Mauri⁴⁶, E. Maurice^{8,b}, B. Maurin⁴⁵,
 M. McCann^{57,44}, A. McNab⁵⁸, R. McNulty¹⁴, J.V. Mead⁵⁶, B. Meadows⁶¹, C. Meaux⁷,
 N. Meinert⁷¹, D. Melnychuk³², M. Merk²⁸, A. Merli^{22,q}, E. Michielin²⁴, M. Mikhasenko⁴⁴,
 D.A. Milanese⁷⁰, E. Millard⁵², M.-N. Minard⁵, L. Minzoni^{17,g}, D.S. Mitzel¹³, A. Mogini⁹,
 R.D. Moise⁵⁷, T. Mombächer¹¹, I.A. Monroy⁷⁰, S. Monteil⁶, M. Morandin²⁴, G. Morello¹⁹,
 M.J. Morello^{25,t}, J. Moron³¹, A.B. Morris⁷, R. Mountain⁶³, H. Mu³, F. Muheim⁵⁴,
 M. Mukherjee⁶⁹, M. Mulder²⁸, C.H. Murphy⁵⁹, D. Murray⁵⁸, A. Mödden¹¹, D. Müller⁴⁴,
 J. Müller¹¹, K. Müller⁴⁶, V. Müller¹¹, P. Naik⁵⁰, T. Nakada⁴⁵, R. Nandakumar⁵³, A. Nandi⁵⁹,
 T. Nanut⁴⁵, I. Nasteva², M. Needham⁵⁴, N. Neri^{22,q}, S. Neubert¹³, N. Neufeld⁴⁴,
 R. Newcombe⁵⁷, T.D. Nguyen⁴⁵, C. Nguyen-Mau^{45,n}, S. Nieswand¹⁰, R. Niet¹¹, N. Nikitin³⁵,
 N.S. Nolte⁴⁴, D.P. O'Hanlon¹⁶, A. Oblakowska-Mucha³¹, V. Obraztsov⁴⁰, S. Ogilvy⁵⁵,
 R. Oldeman^{23,f}, C.J.G. Onderwater⁷⁴, J. D. Osborn⁸⁰, A. Ossowska³⁰, J.M. Otalora Goicochea²,
 T. Ovsiannikova³⁴, P. Owen⁴⁶, A. Oyanguren⁷⁸, P.R. Pais⁴⁵, T. Pajero^{25,t}, A. Palano¹⁵,
 M. Palutan¹⁹, G. Panshin⁷⁷, A. Papanestis⁵³, M. Pappagallo⁵⁴, L.L. Pappalardo^{17,g},
 W. Parker⁶², C. Parkes^{58,44}, G. Passaleva^{18,44}, A. Pastore¹⁵, M. Patel⁵⁷, C. Patrignani^{16,e},
 A. Pearce⁴⁴, A. Pellegrino²⁸, G. Penso²⁷, M. Pepe Altarelli⁴⁴, S. Perazzini¹⁶, D. Pereima³⁴,
 P. Perret⁶, L. Pescatore⁴⁵, K. Petridis⁵⁰, A. Petrolini^{20,h}, A. Petrov⁷⁵, S. Petrucci⁵⁴,

M. Petruzzo^{22,q}, B. Pietrzyk⁵, G. Pietrzyk⁴⁵, M. Pikies³⁰, M. Pili⁵⁹, A. Pilloni^{72,20}, D. Pinci²⁷, J. Pinzino⁴⁴, F. Pisani⁴⁴, A. Piucci¹³, V. Placinta³³, S. Playfer⁵⁴, J. Plews⁴⁹, M. Plo Casasus⁴³, F. Polci⁹, M. Poli Lener¹⁹, M. Poliakova⁶³, A. Poluektov⁷, N. Polukhina^{76,c}, I. Polyakov⁶³, E. Polycarpo², G.J. Pomery⁵⁰, S. Ponce⁴⁴, A. Popov⁴⁰, D. Popov⁴⁹, S. Poslavskii⁴⁰, E. Price⁵⁰, C. Prouve⁴³, V. Pugatch⁴⁸, A. Puig Navarro⁴⁶, H. Pullen⁵⁹, G. Punzi^{25,p}, W. Qian⁶⁶, J. Qin⁶⁶, R. Quagliani⁹, B. Quintana⁶, N.V. Raab¹⁴, B. Rachwal³¹, J.H. Rademacker⁵⁰, M. Rama²⁵, M. Ramos Pernas⁴³, M.S. Rangel², F. Ratnikov^{37,38}, G. Raven²⁹, M. Ravonel Salzgeber⁴⁴, M. Reboud⁵, F. Redi⁴⁵, S. Reichert¹¹, A.C. dos Reis¹, F. Reiss⁹, C. Remon Alepuz⁷⁸, Z. Ren³, V. Renaudin⁵⁹, S. Ricciardi⁵³, S. Richards⁵⁰, K. Rinnert⁵⁶, P. Robbe⁸, A. Robert⁹, A.B. Rodrigues⁴⁵, E. Rodrigues⁶¹, J.A. Rodriguez Lopez⁷⁰, M. Roehrken⁴⁴, S. Roiser⁴⁴, A. Rollings⁵⁹, V. Romanovskiy⁴⁰, A. Romero Vidal⁴³, J.D. Roth⁸⁰, M. Rotondo¹⁹, M.S. Rudolph⁶³, T. Ruf⁴⁴, J. Ruiz Vidal⁷⁸, J.J. Saborido Silva⁴³, N. Sagidova⁴¹, B. Saitta^{23,f}, V. Salustino Guimaraes⁶⁵, C. Sanchez Gras²⁸, C. Sanchez Mayordomo⁷⁸, B. Sanmartin Sedes⁴³, R. Santacesaria²⁷, C. Santamarina Rios⁴³, M. Santimaria^{19,44}, E. Santovetti^{26,j}, G. Sarpis⁵⁸, A. Sarti^{19,k}, C. Satriano^{27,s}, A. Satta²⁶, M. Saur⁶⁶, D. Savrina^{34,35}, S. Schael¹⁰, M. Schellenberg¹¹, M. Schiller⁵⁵, H. Schindler⁴⁴, M. Schmelling¹², T. Schmelzer¹¹, B. Schmidt⁴⁴, O. Schneider⁴⁵, A. Schopper⁴⁴, H.F. Schreiner⁶¹, M. Schubiger²⁸, S. Schulte⁴⁵, M.H. Schune⁸, R. Schwemmer⁴⁴, B. Sciascia¹⁹, A. Sciubba^{27,k}, A. Semennikov³⁴, E.S. Sepulveda⁹, A. Sergi^{49,44}, N. Serra⁴⁶, J. Serrano⁷, L. Sestini²⁴, A. Seuthe¹¹, P. Seyfert⁴⁴, M. Shapkin⁴⁰, T. Shears⁵⁶, L. Shekhtman^{39,x}, V. Shevchenko⁷⁵, E. Shmanin⁷⁶, B.G. Siddi¹⁷, R. Silva Coutinho⁴⁶, L. Silva de Oliveira², G. Simi^{24,o}, S. Simone^{15,d}, I. Skiba¹⁷, N. Skidmore¹³, T. Skwarnicki⁶³, M.W. Slater⁴⁹, J.G. Smeaton⁵¹, E. Smith¹⁰, I.T. Smith⁵⁴, M. Smith⁵⁷, M. Soares¹⁶, I. Soares Lavra¹, M.D. Sokoloff⁶¹, F.J.P. Soler⁵⁵, B. Souza De Paula², B. Spaan¹¹, E. Spadaro Norella^{22,q}, P. Spradlin⁵⁵, F. Stagni⁴⁴, M. Stahl¹³, S. Stahl⁴⁴, P. Steffko⁴⁵, S. Stefkova⁵⁷, O. Steinkamp⁴⁶, S. Stemmler¹³, O. Stenyakin⁴⁰, M. Stepanova⁴¹, H. Stevens¹¹, A. Stocchi⁸, S. Stone⁶³, S. Stracka²⁵, M.E. Stramaglia⁴⁵, M. Straticic³³, U. Straumann⁴⁶, S. Strokov⁷⁷, J. Sun³, L. Sun⁶⁸, Y. Sun⁶², K. Swientek³¹, A. Szabelski³², A. Szczepaniak^{81,ac}, T. Szumlak³¹, M. Szymanski⁶⁶, S. T'Jampens⁵, Z. Tang³, T. Tekampe¹¹, G. Tellarini¹⁷, F. Teubert⁴⁴, E. Thomas⁴⁴, J. van Tilburg²⁸, M.J. Tilley⁵⁷, V. Tisserand⁶, M. Tobin⁴, S. Tolka⁴⁴, L. Tomassetti^{17,g}, D. Tonelli²⁵, D.Y. Tou⁹, E. Tournefier⁵, M. Traill⁵⁵, M.T. Tran⁴⁵, A. Trisovic⁵¹, A. Tsaregorodtsev⁷, G. Tuci^{25,44,p}, A. Tully⁵¹, N. Tuning²⁸, A. Ukleja³², A. Usachov⁸, A. Ustyuzhanin^{37,38}, U. Uwer¹³, A. Vagner⁷⁷, V. Vagnoni¹⁶, A. Valassi⁴⁴, S. Valat⁴⁴, G. Valenti¹⁶, H. Van Hecke⁸², C.B. Van Hulse¹⁴, A. Vasiliev⁴⁰, R. Vazquez Gomez⁴⁴, P. Vazquez Regueiro⁴³, S. Vecchi¹⁷, M. van Veghel²⁸, J.J. Velthuis⁵⁰, M. Veltri^{18,r}, A. Venkateswaran⁶³, M. Vernet⁶, M. Veronesi²⁸, M. Vesterinen⁵², J.V. Viana Barbosa⁴⁴, D. Vieira⁶⁶, M. Vieites Diaz⁴³, H. Viemann⁷¹, X. Vilasis-Cardona^{42,m}, A. Vitkovskiy²⁸, M. Vitti⁵¹, V. Volkov³⁵, A. Vollhardt⁴⁶, D. Vom Bruch⁹, B. Voneki⁴⁴, A. Vorobyev⁴¹, V. Vorobyev^{39,x}, N. Voropaev⁴¹, J.A. de Vries²⁸, C. Vázquez Sierra²⁸, R. Waldi⁷¹, J. Walsh²⁵, J. Wang⁴, J. Wang³, M. Wang³, Y. Wang⁶⁹, Z. Wang⁴⁶, D.R. Ward⁵¹, H.M. Wark⁵⁶, N.K. Watson⁴⁹, D. Websdale⁵⁷, A. Weiden⁴⁶, C. Weisser⁶⁰, M. Whitehead¹⁰, G. Wilkinson⁵⁹, M. Wilkinson⁶³, I. Williams⁵¹, M.R.J. Williams⁵⁸, M. Williams⁶⁰, T. Williams⁴⁹, F.F. Wilson⁵³, M. Winn⁸, W. Wislicki³², M. Witek³⁰, G. Wormser⁸, S.A. Wotton⁵¹, K. Wyllie⁴⁴, D. Xiao⁶⁹, Y. Xie⁶⁹, H. Xing⁶⁷, A. Xu³, L. Xu³, M. Xu⁶⁹, Q. Xu⁶⁶, Z. Xu³, Z. Xu⁵, Z. Yang³, Z. Yang⁶², Y. Yao⁶³, L.E. Yeomans⁵⁶, H. Yin⁶⁹, J. Yu^{69,aa}, X. Yuan⁶³, O. Yushchenko⁴⁰, K.A. Zarebski⁴⁹, M. Zavertyaev^{12,c}, M. Zeng³, D. Zhang⁶⁹, L. Zhang³, S. Zhang³, W.C. Zhang^{3,z}, Y. Zhang⁴⁴, A. Zhelezov¹³, Y. Zheng⁶⁶, X. Zhu³, V. Zhukov^{10,35}, J.B. Zonneveld⁵⁴, S. Zucchelli^{16,e}.

¹Centro Brasileiro de Pesquisas Físicas (CBPF), Rio de Janeiro, Brazil

²Universidade Federal do Rio de Janeiro (UFRJ), Rio de Janeiro, Brazil

³Center for High Energy Physics, Tsinghua University, Beijing, China

⁴Institute Of High Energy Physics (ihep), Beijing, China

- ⁵ *Univ. Grenoble Alpes, Univ. Savoie Mont Blanc, CNRS, IN2P3-LAPP, Annecy, France*
- ⁶ *Université Clermont Auvergne, CNRS/IN2P3, LPC, Clermont-Ferrand, France*
- ⁷ *Aix Marseille Univ, CNRS/IN2P3, CPPM, Marseille, France*
- ⁸ *LAL, Univ. Paris-Sud, CNRS/IN2P3, Université Paris-Saclay, Orsay, France*
- ⁹ *LPNHE, Sorbonne Université, Paris Diderot Sorbonne Paris Cité, CNRS/IN2P3, Paris, France*
- ¹⁰ *I. Physikalisches Institut, RWTH Aachen University, Aachen, Germany*
- ¹¹ *Fakultät Physik, Technische Universität Dortmund, Dortmund, Germany*
- ¹² *Max-Planck-Institut für Kernphysik (MPIK), Heidelberg, Germany*
- ¹³ *Physikalisches Institut, Ruprecht-Karls-Universität Heidelberg, Heidelberg, Germany*
- ¹⁴ *School of Physics, University College Dublin, Dublin, Ireland*
- ¹⁵ *INFN Sezione di Bari, Bari, Italy*
- ¹⁶ *INFN Sezione di Bologna, Bologna, Italy*
- ¹⁷ *INFN Sezione di Ferrara, Ferrara, Italy*
- ¹⁸ *INFN Sezione di Firenze, Firenze, Italy*
- ¹⁹ *INFN Laboratori Nazionali di Frascati, Frascati, Italy*
- ²⁰ *INFN Sezione di Genova, Genova, Italy*
- ²¹ *INFN Sezione di Milano-Bicocca, Milano, Italy*
- ²² *INFN Sezione di Milano, Milano, Italy*
- ²³ *INFN Sezione di Cagliari, Monserrato, Italy*
- ²⁴ *INFN Sezione di Padova, Padova, Italy*
- ²⁵ *INFN Sezione di Pisa, Pisa, Italy*
- ²⁶ *INFN Sezione di Roma Tor Vergata, Roma, Italy*
- ²⁷ *INFN Sezione di Roma La Sapienza, Roma, Italy*
- ²⁸ *Nikhef National Institute for Subatomic Physics, Amsterdam, Netherlands*
- ²⁹ *Nikhef National Institute for Subatomic Physics and VU University Amsterdam, Amsterdam, Netherlands*
- ³⁰ *Henryk Niewodniczanski Institute of Nuclear Physics Polish Academy of Sciences, Kraków, Poland*
- ³¹ *AGH - University of Science and Technology, Faculty of Physics and Applied Computer Science, Kraków, Poland*
- ³² *National Center for Nuclear Research (NCBJ), Warsaw, Poland*
- ³³ *Horia Hulubei National Institute of Physics and Nuclear Engineering, Bucharest-Magurele, Romania*
- ³⁴ *Institute of Theoretical and Experimental Physics NRC Kurchatov Institute (ITEP NRC KI), Moscow, Russia, Moscow, Russia*
- ³⁵ *Institute of Nuclear Physics, Moscow State University (SINP MSU), Moscow, Russia*
- ³⁶ *Institute for Nuclear Research of the Russian Academy of Sciences (INR RAS), Moscow, Russia*
- ³⁷ *Yandex School of Data Analysis, Moscow, Russia*
- ³⁸ *National Research University Higher School of Economics, Moscow, Russia*
- ³⁹ *Budker Institute of Nuclear Physics (SB RAS), Novosibirsk, Russia*
- ⁴⁰ *Institute for High Energy Physics NRC Kurchatov Institute (IHEP NRC KI), Protvino, Russia, Protvino, Russia*
- ⁴¹ *Petersburg Nuclear Physics Institute NRC Kurchatov Institute (PNPI NRC KI), Gatchina, Russia, St.Petersburg, Russia*
- ⁴² *ICCUB, Universitat de Barcelona, Barcelona, Spain*
- ⁴³ *Instituto Galego de Física de Altas Enerxías (IGFAE), Universidade de Santiago de Compostela, Santiago de Compostela, Spain*
- ⁴⁴ *European Organization for Nuclear Research (CERN), Geneva, Switzerland*
- ⁴⁵ *Institute of Physics, Ecole Polytechnique Fédérale de Lausanne (EPFL), Lausanne, Switzerland*
- ⁴⁶ *Physik-Institut, Universität Zürich, Zürich, Switzerland*
- ⁴⁷ *NSC Kharkiv Institute of Physics and Technology (NSC KIPT), Kharkiv, Ukraine*
- ⁴⁸ *Institute for Nuclear Research of the National Academy of Sciences (KINR), Kyiv, Ukraine*
- ⁴⁹ *University of Birmingham, Birmingham, United Kingdom*
- ⁵⁰ *H.H. Wills Physics Laboratory, University of Bristol, Bristol, United Kingdom*
- ⁵¹ *Cavendish Laboratory, University of Cambridge, Cambridge, United Kingdom*
- ⁵² *Department of Physics, University of Warwick, Coventry, United Kingdom*
- ⁵³ *STFC Rutherford Appleton Laboratory, Didcot, United Kingdom*
- ⁵⁴ *School of Physics and Astronomy, University of Edinburgh, Edinburgh, United Kingdom*

- ⁵⁵ *School of Physics and Astronomy, University of Glasgow, Glasgow, United Kingdom*
- ⁵⁶ *Oliver Lodge Laboratory, University of Liverpool, Liverpool, United Kingdom*
- ⁵⁷ *Imperial College London, London, United Kingdom*
- ⁵⁸ *School of Physics and Astronomy, University of Manchester, Manchester, United Kingdom*
- ⁵⁹ *Department of Physics, University of Oxford, Oxford, United Kingdom*
- ⁶⁰ *Massachusetts Institute of Technology, Cambridge, MA, United States*
- ⁶¹ *University of Cincinnati, Cincinnati, OH, United States*
- ⁶² *University of Maryland, College Park, MD, United States*
- ⁶³ *Syracuse University, Syracuse, NY, United States*
- ⁶⁴ *Laboratory of Mathematical and Subatomic Physics , Constantine, Algeria, associated to ²*
- ⁶⁵ *Pontificia Universidade Católica do Rio de Janeiro (PUC-Rio), Rio de Janeiro, Brazil, associated to ²*
- ⁶⁶ *University of Chinese Academy of Sciences, Beijing, China, associated to ³*
- ⁶⁷ *South China Normal University, Guangzhou, China, associated to ³*
- ⁶⁸ *School of Physics and Technology, Wuhan University, Wuhan, China, associated to ³*
- ⁶⁹ *Institute of Particle Physics, Central China Normal University, Wuhan, Hubei, China, associated to ³*
- ⁷⁰ *Departamento de Física , Universidad Nacional de Colombia, Bogota, Colombia, associated to ⁹*
- ⁷¹ *Institut für Physik, Universität Rostock, Rostock, Germany, associated to ¹³*
- ⁷² *European Centre for Theoretical Studies in Nuclear Physics and Related Areas and Fondazione Bruno Kessler, Villazzano, Italy*
- ⁷³ *Universidad Nacional Autónoma de México, Ciudad de México*
- ⁷⁴ *Van Swinderen Institute, University of Groningen, Groningen, Netherlands, associated to ²⁸*
- ⁷⁵ *National Research Centre Kurchatov Institute, Moscow, Russia, associated to ³⁴*
- ⁷⁶ *National University of Science and Technology “MISIS”, Moscow, Russia, associated to ³⁴*
- ⁷⁷ *National Research Tomsk Polytechnic University, Tomsk, Russia, associated to ³⁴*
- ⁷⁸ *Instituto de Física Corpuscular, Centro Mixto Universidad de Valencia - CSIC, Valencia, Spain, associated to ⁴²*
- ⁷⁹ *H.H. Wills Physics Laboratory, University of Bristol, Bristol, United Kingdom, Bristol, United Kingdom*
- ⁸⁰ *University of Michigan, Ann Arbor, United States, associated to ⁶³*
- ⁸¹ *Indiana University, Bloomington, United States*
- ⁸² *Los Alamos National Laboratory (LANL), Los Alamos, United States, associated to ⁶³*
- ^a *Universidade Federal do Triângulo Mineiro (UFMT), Uberaba-MG, Brazil*
- ^b *Laboratoire Leprince-Ringuet, Palaiseau, France*
- ^c *P.N. Lebedev Physical Institute, Russian Academy of Science (LPI RAS), Moscow, Russia*
- ^d *Università di Bari, Bari, Italy*
- ^e *Università di Bologna, Bologna, Italy*
- ^f *Università di Cagliari, Cagliari, Italy*
- ^g *Università di Ferrara, Ferrara, Italy*
- ^h *Università di Genova, Genova, Italy*
- ⁱ *Università di Milano Bicocca, Milano, Italy*
- ^j *Università di Roma Tor Vergata, Roma, Italy*
- ^k *Università di Roma La Sapienza, Roma, Italy*
- ^l *AGH - University of Science and Technology, Faculty of Computer Science, Electronics and Telecommunications, Kraków, Poland*
- ^m *LIFAELS, La Salle, Universitat Ramon Llull, Barcelona, Spain*
- ⁿ *Hanoi University of Science, Hanoi, Vietnam*
- ^o *Università di Padova, Padova, Italy*
- ^p *Università di Pisa, Pisa, Italy*
- ^q *Università degli Studi di Milano, Milano, Italy*
- ^r *Università di Urbino, Urbino, Italy*
- ^s *Università della Basilicata, Potenza, Italy*
- ^t *Scuola Normale Superiore, Pisa, Italy*
- ^u *Università di Modena e Reggio Emilia, Modena, Italy*
- ^v *H.H. Wills Physics Laboratory, University of Bristol, Bristol, United Kingdom*
- ^w *MSU - Iligan Institute of Technology (MSU-IIT), Iligan, Philippines*
- ^x *Novosibirsk State University, Novosibirsk, Russia*

^y*Sezione INFN di Trieste, Trieste, Italy*

^z*School of Physics and Information Technology, Shaanxi Normal University (SNNU), Xi'an, China*

^{aa}*Physics and Micro Electronic College, Hunan University, Changsha City, China*

^{ab}*Lanzhou University, Lanzhou, China*

^{ac}*Thomas Jefferson National Accelerator Facility, Newport News, United States*

[†]*Deceased*